HHS Public Access

Author manuscript

Adv Mater Technol. Author manuscript; available in PMC 2023 January 01.

Published in final edited form as:

Adv Mater Technol. 2022 January ; 7(1): . doi:10.1002/admt.202100885.

Sonoporation: Past, Present, and Future

Joseph Rich,
Department of Biomedical Engineering, Duke University, Durham, NC, 27708, USA

Zhenhua Tian,
Department of Aerospace Engineering, Mississippi State University, Mississippi State, MS, 39762, USA

Tony Jun Huang
Department of Mechanical Engineering and Materials Science, Duke University, Durham, NC, 27708, USA

Abstract

A surge of research in intracellular delivery technologies is underway with the increased innovations in cell-based therapies and cell reprogramming. Particularly, physical cell membrane permeabilization techniques are highlighted as the leading technologies because of their unique features, including versatility, independence of cargo properties, and high-throughput delivery that is critical for providing the desired cell quantity for cell-based therapies. Amongst the physical permeabilization methods, sonoporation holds great promise and has been demonstrated for delivering a variety of functional cargos, such as biomolecular drugs, proteins, and plasmids, to various cells including cancer, immune, and stem cells. However, traditional bubble-based sonoporation methods usually require special contrast agents. Bubble-based sonoporation methods also have high chances of inducing irreversible damage to critical cell components, lowering the cell viability, and reducing the effectiveness of delivered cargos. To overcome these limitations, several novel non-bubble-based sonoporation mechanisms are under development. This review will cover both the bubble-based and non-bubble-based sonoporation mechanisms being employed for intracellular delivery, the technologies being investigated to overcome the limitations of traditional platforms, as well as perspectives on the future sonoporation mechanisms, technologies, and applications.

Graphical Abstract

tian@ae.msstate.edu; tony.huang@duke.edu.

Conflicts of Interest: T.J.H. has co-founded a start-up company, Ascent Bio-Nano Technologies Inc., to commercialize technologies involving acoustofluidics and acoustic tweezers.

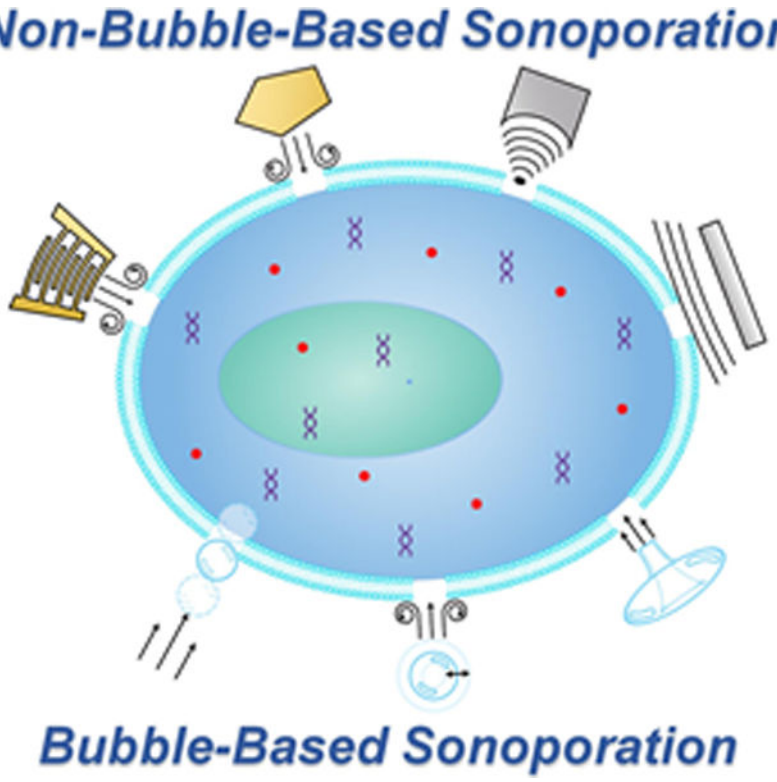

Table of Contents:

This review presents a comprehensive evaluation of the current state of sonoporation research and its advantages and limitations. Particularly, this review covers the current bubble-based sonoporation mechanisms and the novel upcoming non-bubble-based sonoporation mechanisms and their respective technologies that are utilized to enhance intracellular delivery. This review concludes with a perspective on how the field of sonoporation can advance.

Keywords

sonoporation; intracellular delivery; physical permeabilization; acoustics; acoustofluidics

1. Introduction

Cells are marvelous machinery for manufacturing miraculous outputs from a variety of cargos delivered to them. The creation of life itself is founded upon the intracellular delivery of material into a cell. To control what is delivered to cells, various intracellular delivery approaches have been discovered and are under continuous development.[1-22] These recent advances not only contribute to fundamental studies in areas of biology, bioengineering, and medicine, but also benefit several life-changing technologies, such as cell-based therapies, protein therapeutics, vaccines, as well as the reprogramming of cells.[22]

Among the current delivery approaches, the viral vector-based approach is often considered the gold standard for the delivery of nucleic acids.[22] However, due to notable weaknesses

such as biohazards, inconsistent results, and labor-intensive manufacturing,[22-24] physical permeabilization approaches are being pursued,[1-12, 22] including electroporation,[25-26] hydroporation,[27-32] mechanoporation,[25, 32-40] and sonoporation.[41-42] These approaches are noted as advanced due to their high throughputs, cost-effectiveness, and universal nature to deliver a variety of cargos regardless of cell type.[3] Of the physical permeabilization approaches, sonoporation wields great potential and has been demonstrated as an efficacious technology for delivering a variety of functional cargos, such as biomolecular drugs, proteins, and plasmids, to different types of cells, such as cancer, immune, and stem cells.[43-48]

Sonoporation was discovered in the 1980s, a golden age of intracellular delivery, in which quite a few physical permeabilization methods were invented.[49-58] Sonoporation enhances the intracellular delivery of cargos into cells by employing acoustic waves to disrupt their membranes.[22, 59-62] Traditional sonoporation approaches typically rely on ultrasound-induced bubble dynamic behaviors, such as inertial cavitation, non-inertial (stable) cavitation, and bubble translation.[49-52] However, the bubble-based sonoporation approaches usually require special contrast agents,[63-68] which adds a new dimension of complexity and cost to the use of sonoporation. Moreover, bubble-based approaches have a high chance of inducing irreversible cell damage, lowering the cell viability, as well as reducing the effectiveness of delivered cargos.[69-73] Therefore, several novel non-bubble-based sonoporation approaches, such as those based on acoustic radiation force and acoustic streaming-induced shear force, are being developed to overcome the limitations of bubble-based sonoporation approaches. Although there are several review papers on the mechanisms and applications of bubble-based sonoporation,[61-62, 74-88] they have neglected some of the newly developed mechanisms. Therefore, this review article covers recent innovations in bubble-based and especially in non-bubble-based sonoporation. The following Sections review the sonoporation mechanisms, showcase some of the promising technologies of today, and provide thoughtful perspectives on the future of sonoporation.

2. Bubble-based Sonoporation Technologies

Bubble-based sonoporation technologies leverage ultrasound-induced bubble dynamics to open pores on membranes for intracellular delivery. This Section reviews the fundamental mechanisms and critical features of the bubble-based sonoporation technologies. Recent innovations that fuse bubble-based sonoporation and microfluidics are also reviewed.

2.1. Bubble-based mechanisms

To open pores on the cell membrane for intracellular delivery, multiple bubble-based sonoporation mechanisms have been established (see Figure 1), which can be categorized into three groups, including inertial cavitation, stable cavitation, as well as acoustic radiation force-induced cross-membrane bubble translation. In the following, these mechanisms and their key features are reviewed.

2.1.1. Inertial cavitation—Inertial cavitation, one of the first sonoporation mechanisms developed, is typically associated with cavitating bubbles. When acoustic pressures are sufficiently high (*e.g.*, 0.3–1.0 MPa at ~1 MHz)[89-92], bubble collapse can be induced

by acoustic waves thus generating a strong 'jetting' flow (*i.e.*, fluid streaming),[93-94] which can further rupture the membrane of an adjacent cell as illustrated in Figure 1a. In addition to pressure, the inertial cavitation performance is dependent on acoustic wave frequency,[90-92, 95-96] pulse repetition rate,[89] pulse duration,[89] initial bubble radius,[91-92] bubble properties,[90, 95] temperature,[97] fluid properties,[90, 98] wave-type,[99-100] and device energy efficiency.[99-100] Apart from the 'jetting' effect, inertial cavitation is also associated with shock waves generated from the bubble collapse. These shock waves propagate and generate intense fluid streaming, resulting in the perforation of a cell membrane,[72, 94, 101-103] as shown in Figure 1b. However, the strong 'jetting' flow and shock waves have high chances to create non-recoverable cell membrane pores and lead to low cell viability.[69-72] Inertial cavitation also involves other unstable byproducts, such as temperature[104] and reactive oxygen species[105-107] that could influence intracellular delivery and viability.

2.1.2. Stable cavitation—To address the issue of inertial cavitation, several stable cavitation mechanisms (see Figure 1c-e) have been established to better control the process of opening pores on cell membranes.[108-112] These mechanisms typically leverage oscillating bubbles induced by acoustic waves. As shown in Figure 1c, when oscillating bubble-induced fluid streaming applies a strong enough shear stress (~15 to ~5,000 Pa)[61, 111, 113-116] for a long enough duration (microseconds to minutes),[61, 111, 113-116] pores can form on the cell membrane. Unfortunately, this mechanism highly depends on bubble-cell distance[85, 117-119] and bubble size,[79, 85, 120-121] which are difficult to control. On the other hand, when an oscillating bubble is attached on a cell membrane, the bubble expansion (or contraction) can apply forces to push (or pull) the membrane as illustrated in Figure 1d and e. Studies show that this push-pull process can open micropores on the cell membrane for intracellular delivery.[61, 70, 79, 114, 122] However, this mechanism is dependent on successfully attaching bubbles on cell membranes. Usually, it is difficult to attach the same number of bubbles on individual cells.[116, 120, 123]

2.1.3. Acoustic radiation force on bubbles—In addition to inertial and stable cavitation mechanisms, recent studies show that the primary Bjerknes force (*i.e.*, primary acoustic radiation force applied on a bubble) can push a bubble through the cell membrane,[124] as illustrated in Figure 1f. The primary Bjerknes force highly relies on the bubble radius, acoustic impedance, and acoustic energy density.[125-127] By translating a bubble across a cell membrane, the membrane can be temporarily disrupted, thus permitting the diffusion of extracellular cargo into the cell.[79, 124, 128-130]

2.2. Conventional bubble-based technologies

Conventional bubble-based technologies typically leverage sonicating bath systems with similar configurations (in Figure 2a-c) by placing planar or focused acoustic transducers at the bottom or top of a sonicating bath to send acoustic waves to a chamber (*e.g.*, petri dish, Eppendorf tube, or customized chamber) containing both bubbles and cells. For these conventional technologies, acoustic waves transmit to the chamber from the bath, induce bubble dynamic behaviors in the chamber, and further enable sonoporation.

To better understand the mechanisms of conventional sonoporation technologies, Helfield *et al.* investigated the effects of acoustic pressure, frequency, and treatment time.[102] By using an acoustic pressure of 0.5 MPa at 1 MHz, their results (in Figure 2d) only show negligible bubble oscillation. However, with higher acoustic pressures, their results show strong bubble oscillations at 0.8 MPa as well as bubble shell cracking with gas release at 1 MPa. These different bubble dynamic behaviors can also be confirmed from the bubble size histories (Figure 2e), which periodically change due to the applied acoustic waves. Moreover, their response frequency results (Figure 2f) indicate large nonlinear frequency components. By leveraging the acoustic waves-induced shell cracking (*i.e.*, inertial cavitation), they observed the primary adherent cell cytoplasm intake of cargos (*e.g.*, propidium iodide, PI) and more interestingly nucleus intake of cargos (Figure 2g). However, the bubble-based sonoporation may greatly affect cell viability. For example, after an 8 μs burst of acoustic waves with pressures in a range of 0.4-1.6 MPa, the viability can drop to a range of ~55-80%.

Many groups have leveraged conventional bubble-based sonoporation for delivering various cargos into different types of cells. For example, Butto *et al.* utilized 2.5 MHz acoustic waves with peak pressures ranging from 0.6 to 4.8 MPa for inertial cavitation as well as delivering 2 MDa dextran and green fluorescent protein (GFP) to cancer and cardiac cells.[43] They found that high peak negative pressures led to higher delivery efficiency with lower viability, ~40% for cardiac cells and ~70% for cancer cells. Karki *et al.* employed conventional sonoporation with 5-12 seconds of stable cavitation at 2.2 MHz to deliver siRNA to murine T cells.[46] The efficiency of delivering siRNA to murine T cells was approximately ~60% with a viability of ~60%. As found in previous studies, the acoustic wave pressure, frequency, and treatment time can have significant effects on the bubble dynamic behaviors and accordingly the sonoporation mechanism and performance. Therefore, these factors should be considered when using bubble-based sonoporation technologies.

2.3. Recent bubble-based microfluidic technologies

Various bubble-based microfluidic platforms that fuse microfluidics and different bubble-based sonoporation mechanisms have recently been developed to better control cell-bubble interaction as well as achieve better intracellular delivery performance. For example, Meng *et al.* developed a novel stable cavitation-based microfluidic device (Figure 3a), which leverages a microfluidic channel to trap an array of bubbles for sonoporation.[115] In their device, when 107 kHz acoustic waves with pressures in a range of 7.4-64.1 kPa were used, they found strong vortex streaming (Figure 3b) generated from oscillating bubbles could attract and trap cells near the bubble shells. The vortex streaming also increased shear stress (~177 Pa) on cells, thus increasing the membrane permeability. As shown in Figure 3c, after 30-90 s of exposure time, cancer cells pre-stained with Calcein-AM (green) showed PI (red), confirming the enhanced membrane permeability. Through a series of experiments, they found that their device achieved PI delivery efficiency in the range of ~70-90% with viability in a range of ~80-100%. Given these features, their device is still limited by the number of bubbles that it can trap as well as the number of cells trapped by bubble oscillation-induced vortex streaming. In addition to trapping bubbles, Centner *et al.* leveraged a spiral microfluidic channel to enhance cell and bubble residence time in

the sonicating bath region of interest.[131] As shown in Figure 3d and e, their setup can be considered as a modified version of the conventional bubble-based setup in Figure 2, by changing the chamber containing cells to a spiral microfluidic channel with flowing cells. Compared to conventional setups, their device can achieve sonoporation for cells in a continuous flow for potential high-throughput applications.

In addition to technologies directly leveraging cavitating bubbles, Meng *et al.* demonstrated a technology (Figure 3f) that uses surface acoustic wave-based acoustic tweezers to precisely move a bubble to a target cell and then enable inertial bubble cavitation for sonoporation.[132] As shown in Figure 3g, by tuning input phases and amplitudes from multiple interdigital transducers, the controlled standing waves translated a bubble along a complex path to the desired location. Given that their device employed high-frequency surface acoustic waves, which are typically difficult to induce cavitation,[99-100] Meng *et al.* leveraged an intense pulse of 24 MHz surface acoustic waves to successfully induce inertial cavitation. After sonoporation, PI (red) successfully entered the transiently porous cell (see Figure 3g). They found their approach could achieve an efficiency of ~80% and a viability of ~90% for delivering PI to cancer cells. Although their technology is useful for controlled sonoporation of a target cell adhered on a substrate, it may not be suitable for high-throughput applications.

3. Non-bubble-based Sonoporation Technologies

Recently, there has been a rising interest in developing non-bubble-based sonoporation technologies to address the challenges associated with bubble-based sonoporation. This section will review the non-bubble-based sonoporation mechanisms together with their related forces for enhancing membrane permeability, such as acoustic radiation force applied on cells and shear force induced by acoustic streaming. Afterwards, representative non-bubble-based sonoporation technologies are reviewed in four different categories, which are based on the acoustic wave types (such as bulk acoustic waves, Lamb waves, and surface acoustic waves), wave frequency ranges, and particular attributes (*e.g.*, high-throughput, localized, and *in vivo* sonoporation).

3.1. Non-bubble-based mechanisms

When acoustic waves propagate in a fluid containing cells, these cells experience both the acoustic radiation force and the acoustic streaming-induced shear force.[133-138] These forces can increase the membrane stress to thereby open pores on the cell membrane. For cells adhered on substrates, the energy of acoustic waves propagating through substrates can also apply forces on cells and further contribute to the membrane stress.[116] Figure 4 provides schematics for different non-bubble-based sonoporation mechanisms, which leverage the aforementioned forces in different ways for opening pores on cell membranes.

Figure 4a-c illustrate non-bubble-based sonoporation mechanisms that utilize the primary acoustic radiation force, which mainly depends on the cell radius, the acoustic contrast factor, and the acoustic potential gradient.[127] More details of the acoustic radiation force and its capabilities can be found in literature elsewhere.[126-127, 133, 139-142] As illustrated in Figure 4a, the acoustic radiation force generated from a bulk acoustic wave transducer (gray

area) pushes a cell through a constricting nozzle orifice.[143] As a cell is ejected from the nozzle, the combined acoustic radiation force with the reaction force from the constricting nozzle can open pores on the cell membrane. In addition to pushing cells through a nozzle, recently, a bulk acoustic wave resonator leveraged acoustic radiation forces to push cells to a pressure node located at the center of the microfluidic channel,[144-145] as illustrated in Figure 4b. The applied forces through acoustic waves increase the membrane stress, further leading to a change in permeability. Figure 4c shows a more recent mechanism based on the acoustic resonator concept, which pushes cells to a pressure node located at the channel wall.[45] As cells are flowing and/or rolling along the channel wall, they experience both forces directly from the applied acoustic waves as well as forces from the membrane-channel wall reaction.

Figure 4d-f illustrate the mechanisms for the sonoporation of cells adhered on substrates by using different types of acoustic waves, such as Lamb waves, surface acoustic waves, and localized bulk acoustic waves. Fundamentals of different wave types can be found in previous studies.[126, 146-147] In these sonoporation mechanisms, the primary acoustic radiation force, the acoustic streaming, as well as the forces applied through the cell-substrate interface could all contribute to the cell membrane stress and the opening of membrane pores. As illustrated in Figure 4d, antisymmetric Lamb waves in the kHz range (or low-frequency flexural waves) generated from a piezoelectric transducer can efficiently propagate along a thin-wall substrate to deliver wave energy to a cell adhered on the substrate for sonoporation.[148] In this mechanism, the cell experiences forces directly applied through the membrane-substrate interface. Moreover, the leaky Lamb waves (*i.e.*, waves that leak into the fluid domain) apply acoustic radiation force on the cell as well as a shear force through the generated fluid streaming. In addition to low-frequency Lamb waves, high-frequency surface acoustic waves can sonoporate cells adhered on a substrate.[149] As illustrated in Figure 4e, the surface acoustic waves generated by an interdigital transducer can propagate on the surface of a piezoelectric substrate[150-151] and deliver acoustic energy to a cell adhered on the substrate. These surface acoustic waves can apply forces on cells through the substrate-cell contact, leaky energy-induced acoustic radiation force, as well as acoustic streaming-induced shear force. More details of surface acoustic waves[126, 138-139, 146-147, 152-157] and acoustic streaming-induced shear forces[126, 133, 139, 158-166] can be found in literature. Figure 4f shows a schematic of a bulk acoustic wave-based mechanism for the sonoporation of a cell adhered on a substrate.[167] Particularly, when the acoustic transducer is small enough, it allows for localized sonoporation of the cell above/near the transducer. To achieve localized sonoporation, some recent studies have also introduced focused high-frequency acoustic waves (Figure 4g) to generate a concentrated acoustic energy beam with enhanced acoustic radiation force to permeabilize a target cell without influencing neighboring cells.[168-172].

Figure 4h and i illustrate non-bubble-based sonoporation mechanisms that rely on acoustic streaming. As shown in Figure 4h, hyper-frequency (>1 GHz)[173-178] bulk acoustic waves generated from a GHz acoustic resonator can generate intense acoustic streaming, which applies a shear force on a cell adhered on a substrate. Studies show that the applied shear force is strong enough to deform the cell and enhance the membrane permeability.[178] On the other hand, surface acoustic waves generated by an interdigital transducer (*e.g.*, tapered

or focused transducer) can also enable strong surface acoustic wave streaming (Figure 4i) and, therefore, apply a strong shear force to enhance the membrane permeability.[179-180]

In addition to the aforementioned non-bubble-based mechanisms, the acoustic energy dissipation can lead to thermal energy, influencing the sonoporation performance. For example, the temperature increase may affect the cell viability as well as the cell membrane permeability.[22, 181-185] Therefore, researchers working on sonoporation are suggested to characterize how their acoustic platforms influence the temperature condition as well as how the temperature affects the sonoporation performance. In addition, the sonoporation mechanisms can be used together with other intracellular delivery approaches such as electroporation and viral vector-based approaches.[10, 186-192]

3.2. Low-to-mid-frequency, bulk acoustic wave- and Lamb wave-based technologies

In the low-to-mid frequency range (*e.g.*, < 10 MHz), several sonoporation technologies have recently been developed based on bulk acoustic waves and Lamb waves to achieve intracellular delivery.[45, 143-145, 148] As shown in Figure 5a-d, Belling *et al.* developed a bulk acoustic wave resonator-based sonoporation device, composed of a glass capillary coated with desired cargos and a piezoelectric transducer.[45] The acoustic waves generated by the 3.3 MHz transducer can transmit into the fluid space inside the capillary and form standing acoustic waves, which have a pressure node centered along the capillary wall (Figure 5a). With this feature, the resulted acoustic radiation force can push cells on the capillary wall coated with cargos, as they are flowing through the capillary (Figure 5b). Their studies show that the combination of the applied acoustic radiation force and the reaction force from the cell-wall contact can enhance the membrane permeability as well as enable direct contact between cells and coated cargos. Their results (Figure 5c) show that Cy3-labeled DNA can be successfully delivered to the cytoplasm and even the nucleus. To confirm the nuclear membrane rupture, the nuclear localization signal green fluorescent protein (NLS-GFP) and 4,6-diamidino-2-phenylindole (DAPI) are used. Their results (Figure 5d) show the spread of the NLS-GFP in post-treatment mouse embryonic fibroblasts, indicating the rupture of the nuclear envelope. Surprisingly, even with the nuclear envelope mechanically perturbed, the viability of this technology is >75% for primary cells, given the negative effects that can come from tampering with the nuclear envelope.[193-195] Although this method can achieve high-throughput (~2×10^5 cells/min) intracellular delivery, the eGFP plasmid DNA expression is rather low (<28%) for primary cells. This method shows great potential for moving the field of sonoporation forward as a competitive, high-throughput intracellular delivery platform.

In addition to using bulk acoustic wave-based resonators, Lamb waves in the kHz range have been utilized for sonoporation. Salari *et al.* established a Lamb wave-based sonoporation platform,[148] composed of a piezoelectric disk for generating Lamb waves in a thin glass substrate with a microfluidic chamber (Figure 5e). The glass substrate can efficiently deliver the 96 kHz Lamb wave energy to the microfluidic chamber. The wave energy further leads to a microstreaming environment, which then pulls cargos closer to cells adhered on the substrate and helps endocytosis for enhancing intracellular delivery performance.[148, 196] With an exposure time of 20 minutes, their device can successfully deliver high molecular

weight dextran (500 kDa) to various adherent cell lines (*e.g.*, MDA-MB-231, MCF-7, and PC3 cells) with efficiencies in the range of ~65-85%. This technology is useful for the intracellular delivery to several cells per batch and can be scaled by the size of the chamber; however, it has only been validated for cancer cells adhered on the substrate. It would be valuable to see how this technology applies to primary cells and suspension cells.

3.3. High-frequency, bulk acoustic wave-based, localized technologies

Bulk acoustic waves at high frequencies (*e.g.*, 10 MHz to 1 GHz) have smaller wavelengths and generate higher acoustic radiation forces, compared to the waves in the low-to-mid frequency range. With those features, several technologies based on high-frequency bulk acoustic waves have been developed for sonoporation.[167, 169-170] These technologies typically leverage customized transducers to generate strong localized bulk acoustic waves, which achieve localized, precise delivery of different cargos into individual cells. For example, Theo *et al.* developed piezoelectric micropillars, which were made of lead magnesium niobate-lead titanate (PMN-PT) with microelectrodes, for achieving localized sonoporation of target cells in small areas above the piezoelectric micropillars (Figure 6a and b).[167] Their piezoelectric micropillars can emit 30 MHz acoustic waves with a pressure of up to 0.4 MPa to oscillate the cells. When the applied pressure is above the threshold pressure (~0.12 MPa),[167] their approach can lead to cell membrane failure and, therefore, enhance the membrane permeability for intracellular delivery. As proved by their experimental result (Figure 6c), quantum dots can be successfully delivered to cells only in the local areas above piezoelectric micropillars.

In addition to piezoelectric micropillars, customized ultrasonic transducers (Figure 6d and e) based on curved $LiNbO_3$ piezoelectric materials have recently been developed to generate focused high-frequency (~150 MHz) acoustic waves for single-cell sonoporation.[169-170] Yoon *et al.* showed that their developed ultrasonic transducer can concentrate acoustic energy in a narrow beam, whose diameter was smaller than the size of a cell, to achieve single-cell sonoporation without disrupting the membrane of neighboring cells. Moreover, by using a 3D translation stage, they can freely move the ultrasonic beam to any desired location for sonoporation. As shown in Figure 6f, their approach can deliver two different types of cargos to two neighboring cells, through a cell-by-cell manner. The precision that their sonoporation device achieves can potentially benefit the reprogramming of induced pluripotent stem cells into different types of cells within the same cell culture plate.

3.4. Hyper-frequency, bulk acoustic wave-based streaming technologies

Another novel sonoporation technology worth noting is the hyper-frequency (*e.g.*, >1 GHz) bulk acoustic wave-based streaming. The hyper-frequency bulk acoustic waves are generated by GHz acoustic resonators, which are nanofabricated multilayered structures with thin electrodes, a piezoelectric layer, and reflector layers (see Figure 7a and b).[173, 177-178] Guo *et al.* found that the generated hyper-frequency acoustic waves could lead to strong acoustic streaming, which further applied shear forces on cells attached on a substrate to change the membrane stress and induce cell deformation.[178] Because of the membrane stress change, their technology can increase the membrane permeability for intracellular delivery. By periodically applying hyper-frequency acoustic waves (1.64 GHz frequency

and 50% duty cycle) for 10 min, the GHz acoustic resonators can successfully deliver high-molecular-weight dextran (40 kDa) to cancer cells adhered on a substrate (Figure 7c) with the delivery efficiency of ~47% and viability of ~70%. However, this small-size GHz acoustic resonator can only sonoporate cells near the resonator. To address this limitation, an array of GHz acoustic resonators has been used with each resonator placed in a well of a 96-well plate.[173]

3.5. High-frequency, surface acoustic wave-based technologies

Surface acoustic waves in the frequency range of 10's MHz to 10's GHz[150, 197-201] have gained increased attention due to their extensive value in manipulation, separation, and concentration of organisms,[202-204] cells,[205-218] particles,[140, 212, 215, 219-229] and nanomaterials.[230-232] Recently, surface acoustic waves have been leveraged to develop various technologies for sonoporation.[132, 149, 179-180, 233] These technologies usually apply acoustic radiation force and acoustic streaming-induced shear force on cells for increasing the permeability. Figure 8a shows one of the recently developed surface acoustic wave-based permeabilization technologies that can achieve acoustically-mediated delivery to cells attached to a solid substrate.[149] In this technology, surface acoustic waves are generated from a straight interdigital transducer and travel along a piezoelectric ($LiNbO_3$) wafer. These waves can propagate to the fluid domain in a well plate by transmitting through a fluid couplant layer and the plate's glass bottom. Hence, for cells adhered on the glass bottom, they are subjected to both acoustic radiation force and shear force induced by acoustic streaming, which can increase the membrane permeability. Through experiments, Ramesan *et al.* found that the membrane quickly resealed itself after acoustic treatment, contributing to the high cell viability (>97%). By using 10 MHz surface acoustic wave and an exposure time of 30 seconds to 10 min, they found this surface acoustic wave-based technology exhibited the ability to deliver siRNA to cells with ~40% delivery efficiency. Moreover, the authors point out that the delivery mechanism for this surface acoustic wave-based technology is not based on endocytosis pathways, due to the lack of overlap (Figure 8b) between the lysosomes and the delivered siRNA in the cytosol, and that the delivery mechanism is based on creating temporary gaps in the membrane, rather than large irreversible pores.

In addition to using surface acoustic waves generated from a straight interdigital transducer, Ramesan *et al.* leveraged a focused elliptical single phase unidirectional transducer to generate focused surface acoustic waves with concentrated energy for the permeabilization of cells suspended in a glass well plate (see Figure 8c).[179] By using 30 MHz surface acoustic waves with an exposure time of 10 min, this platform can deliver siRNA to cancer cells by temporarily reorganizing the cell membrane, to achieve ~80% gene knockdown efficiency and ~91% viability. Moreover, their experimental results (Figure 8d) confirm that the delivery mechanism is not wholly dependent on the endocytic uptake process, due to the low overlap between the lysosomes and the siRNA distributed in the cytosol.

Besides *in vitro* acoustically-mediated permeabilization, Ramesan *et al.* recently have demonstrated the feasibility of surface acoustic wave technologies for *in vivo* applications.[233] Figure 8e depicts their setup for using surface acoustic waves to facilitate the delivery

of drugs to cells in the mucosal tissue. In this setup, a layer of drug is coated on the piezoelectric wafer, which is then pressed onto the tissue. The surface acoustic wave energy can leak into the tissue, induce cell membrane stress, and further enhance drug delivery. By controlling the input voltage, frequency (17-55 MHz), and exposure time (10-40 s), they found the drug delivery penetration depth could be managed in a range of 0-1,000 μm for delivering the optimal dose to the epithelium or mucosa region. Their experimental results (Figure 8f) show that the fluorescein isothiocyanate (FITC, 20-70 kDa) labeled dextran could penetrate the porcine lip tissue approximately 600 μm and achieve ~40-90% delivery efficiency.

To further achieve intracellular delivery for cells in continuous flow, Kamenac *et al.* have recently established a device, which uses acoustic vortex streaming generated by traveling surface acoustic waves in a microfluidic channel (Figure 9a and b).[180] As cells flow through the channel, they are subjected to both the shear forces applied through acoustic vortex streaming and the hydrodynamic shear forces induced by the Y-shaped microfluidic channel. These forces can open pores on cell membranes and enhance the intracellular delivery of a variety of cargos (Figure 9c). Moreover, their study shows that the membrane pores can seal within 1 min post sonoporation. With their optimal operation parameters (surface acoustic wave frequencies in a range of 80.3-82.3 MHz, a flow rate of 80 μL/min, and an exposure time of 2 min), the delivery of FITC-labeled dextran (10 kDa) and eGFP (27 kDa) can be improved by 3-fold and 6-fold, respectively. This technology shows its strengths by delivering genetic materials to cancer cells in a continuous flow. It would be valuable to see if this technology could be applied to primary cells. With the success of using acoustic streaming induced by 80 MHz surface acoustic waves for intracellular delivery, we envision that the potential of using acoustic streaming induced by hyper-frequency >1 GHz surface acoustic waves[150, 197-201] for sonoporation is very plausible.

4. Conclusion and Outlooks

Sonoporation technologies have been rapidly evolving in recent years, with the increasing need for vector-free physical permeabilization approaches for various applications, such as induced pluripotent stem cell regenerative therapies, cancer immunotherapies, and drug delivery.[1-12, 22] This article reviews current sonoporation technologies in two categories: bubble-based and non-bubble-based sonoporation. Their mechanisms, representative platforms, and key capabilities are reviewed with more efforts on recent bubble-based microfluidic and non-bubble-based sonoporation technologies. Multiple bubble-based sonoporation technologies have been established to control cell-bubble interaction as well as achieve better intracellular delivery performance, but these technologies often require the use of special contrast agents, are often dependent on bubble to cell distance, and are dependent on the number of bubbles to cells, which can be difficult to control. Therefore, there has been a push for developing advanced non-bubble-based sonoporation technologies to precisely engineer the acoustic forces to achieve high-throughput, viable sonoporation. Nevertheless, there are several drawbacks that must be overcome in order for sonoporation to attain its potential as a competitive intracellular delivery platform.

Primarily, a deeper understanding and establishment of theoretical models of sonoporation platforms is essential to applying optimized acoustic wave-induced forces to effectively achieve intracellular delivery. Although progress has been made in the past couple of decades in developing theoretical models for understanding the different types of forces applied by bubble-based[234-240] and non-bubble-based[133, 142, 158, 161, 241-243] acoustic waves, there are still several unknowns that need to be addressed. There are limited in-depth theoretical understandings of the cellular response (*e.g.*, stress and deformation of the cell membrane) to the forces applied by the recent non-bubble-based technologies, which are crucial to predicting and developing efficient sonoporation platforms. It would also be valuable to understand how the contents inside the cells are influenced by acoustic waves. In addition, theoretical studies on how the acoustic waves affect the transport of cargos into the transiently porous cell are crucial to understanding the interplay between acoustic waves and intracellular delivery. The aforementioned theoretical studies will be invaluable in guiding the development of future sonoporation platforms.

Next, a more thorough experimental investigation of the potential byproducts of sonoporation is needed to more accurately identify the underlying mechanism of non-bubble-based sonoporation platforms. Particularly, a thorough investigation should be undertaken for the kinetics of pore formation and repair with sonoporation, for the thermodynamics of the acoustic forces on the cell membrane, and for any other sonoporation induced intracellular delivery pathway, such as endocytosis. These experiments will serve the sonoporation and intracellular delivery community by laying the foundation for future sonoporation developers.

Finally, it is essential for sonoporation platforms to demonstrate versatility in practical applications. These include, but aren't limited to, applications such as precise *in vitro* biofabrication of regenerative tissue constructs from induced pluripotent or mesenchymal stem cells, high-throughput *ex vivo* immune cell or hematopoietic stem cell therapy generation, and novel non-bubble-based non-invasive controlled drug delivery *in vivo*. With the established sonoporation theoretical models, novel acoustic metamaterials that can control acoustic waves in the subwavelength scale, and clever engineering and designing of acoustic transducers, these platforms could come to fruition.

As summarized above, by shifting the research focus from conventional bubble-based sonoporation technologies to advanced bubble-based microfluidic and non-bubble-based sonoporation technologies, multiple limitations of conventional technologies can be addressed and critical capabilities (such as single-cell sonoporation, high-throughput intracellular delivery, and *in vivo* drug delivery with controlled penetration depth) can be achieved. Although these recent advances are still in their infancy, we anticipate that future iterations of bubble-based microfluidic and non-bubble-based sonoporation approaches will lead to multiple highly competitive and marketable physical permeabilization-based intracellular delivery technologies. In the long run, the development of sonoporation platforms can benefit both fundamental biomedical and biological research and various applications such as cell reprogramming, cell-based therapy, and controlled drug delivery.

Acknowledgements

We acknowledge the support from the National Science Foundation (CMMI-2104526 and CMMI-2104295) and the National Institutes of Health (R01GM141055, R01GM132603, and R01GM135486). This material is based upon work supported by the National Science Foundation Graduate Research Fellowship under Grant No. 1644868.

Biography

Joseph Rich is currently pursuing a Ph.D. in Biomedical Engineering at Duke University under the supervision of Professor Tony Jun Huang. He received his B.Sc. in chemical engineering from Brigham Young University in 2020. His research interests include acoustofluidics, sonoporation, drug and gene delivery, and micro/nano systems for biomedical diagnostics and therapeutics.

Zhenhua Tian is an Assistant Professor at the Department of Aerospace Engineering at Mississippi State University. He received his Ph.D. degree in Mechanical Engineering from the University of South Carolina in 2015. He then worked as a Postdoctoral Associate in the Mechanical Engineering and Materials Science Department at Duke University from 2016 to 2019. His research interests include acoustic tweezers, structural health monitoring, ultrasonic imaging, and smart materials and structures.

Tony Jun Huang is the William Bevan Distinguished Professor at the Department of Mechanical Engineering and Materials Science (MEMS) at Duke University. Previously he was a Professor and The Huck Distinguished Chair in Bioengineering Science and Mechanics at The Pennsylvania State University. He received his Ph.D. degree in Mechanical and Aerospace Engineering from the University of California, Los Angeles (UCLA) in 2005. His research interests are in the fields of acoustofluidics, optofluidics, and micro/nano systems for biomedical diagnostics and therapeutics.

References

[1]. Meacham JM, Durvasula K, Degertekin FL, Fedorov AG, J. Lab. Autom 2013, 19, 1. [PubMed: 23813915]

[2]. Lakshmanan S, Gupta GK, Avci P, Chandran R, Sadasivam M, Jorge AES, Hamblin MR, Adv. Drug Delivery Rev 2014, 71, 98.

[3]. Stewart MP, Sharei A, Ding X, Sahay G, Langer R, Jensen KF, Nature 2016, 538, 183. [PubMed: 27734871]

[4]. Zhang Y, Yu J, Bomba HN, Zhu Y, Gu Z, Chem. Rev 2016, 116, 12536. [PubMed: 27680291]

[5]. Brooks J, Minnick G, Mukherjee P, Jaberi A, Chang L, Espinosa HD, Yang R, Small 2020, 16, 2004917.

[6]. Sun M, Duan X, Nanotechnol. Precis. Eng 2020, 3, 18.

[7]. Duckert B, Vinkx S, Braeken D, Fauvart M, J. Controlled Release 2021, 330, 963.

[8]. Hur J, Chung AJ, Adv. Sci 2021, 8, 2004595.

[9]. Kumar ARK, Shou Y, Chan B, Tay KL,A, Adv. Mater 2021, 33, 2007421.

[10]. Morshedi Rad D, Alsadat Rad M, Razavi Bazaz S, Kashaninejad N, Jin D, Ebrahimi Warkiani M, Adv. Mater 2021, 33, 2005363.

[11]. Harizaj A, De Smedt SC, Lentacker I, Braeckmans K, Expert Opin. Drug Delivery 2021, 18, 229.

[12]. Raes L, De Smedt SC, Raemdonck K, Braeckmans K, Biotechnol. Adv 2021, 49, 107760. [PubMed: 33932532]

[13]. Peer D, Karp JM, Hong S, Farokhzad OC, Margalit R, Langer R, Nat. Nanotechnol 2007, 2, 751. [PubMed: 18654426]

[14]. Ganta S, Devalapally H, Shahiwala A, Amiji M, J. Controlled Release 2008, 126, 187.

[15]. Prokop A, Davidson JM, J. Pharm. Sci 2008, 97, 3518. [PubMed: 18200527]

[16]. Mintzer MA, Simanek EE, Chem. Rev 2009, 109, 259. [PubMed: 19053809]

[17]. Yoo J-W, Irvine DJ, Discher DE, Mitragotri S, Nat. Rev. Drug Discovery 2011, 10, 521. [PubMed: 21720407]

[18]. Torchilin VP, Nat. Rev. Drug Discovery 2014, 13, 813. [PubMed: 25287120]

[19]. Blanco E, Shen H, Ferrari M, Nat. Biotechnol 2015, 33, 941. [PubMed: 26348965]

[20]. Yang J, Zhang Q, Chang H, Cheng Y, Chem. Rev 2015, 115, 5274. [PubMed: 25944558]

[21]. Wang H-X, Li M, Lee CM, Chakraborty S, Kim H-W, Bao G, Leong KW, Chem. Rev 2017, 117, 9874. [PubMed: 28640612]

[22]. Stewart MP, Langer R, Jensen KF, Chem. Rev 2018, 118, 7409. [PubMed: 30052023]

[23]. Karra D, Dahm R, J. Neurosci 2010, 30, 6171. [PubMed: 20445041]

[24]. van der Loo JCM, Wright JF, Hum. Mol. Genet 2016, 25, R42. [PubMed: 26519140]

[25]. Ding X, Stewart M, Sharei A, Weaver JC, Langer RS, Jensen KF, Nat. Biomed. Eng 2017, 1, 0039. [PubMed: 28932622]

[26]. Shokouhi A-R, Aslanoglou S, Nisbet D, Voelcker NH, Elnathan R, Mater. Horiz 2020, 7, 2810.

[27]. Kang G, Carlson DW, Kang TH, Lee S, Haward SJ, Choi I, Shen AQ, Chung AJ, ACS Nano 2020, 14, 3048. [PubMed: 32069037]

[28]. Hur J, Park I, Lim KM, Doh J, Cho S-G, Chung AJ, ACS Nano 2020, 14, 15094. [PubMed: 33034446]

[29]. Kizer ME, Deng Y, Kang G, Mikael PE, Wang X, Chung AJ, Lab on a Chip 2019, 19, 1747. [PubMed: 30964485]

[30]. Jarrell JA, Twite AA, Lau KHWJ, Kashani MN, Lievano AA, Acevedo J, Priest C, Nieva J, Gottlieb D, Pawell RS, Sci. Rep 2019, 9, 3214. [PubMed: 30824814]

[31]. Deng Y, Kizer M, Rada M, Sage J, Wang X, Cheon D-J, Chung AJ, Nano Lett. 2018, 18, 2705. [PubMed: 29569926]

[32]. Liu A, Islam M, Stone N, Varadarajan V, Jeong J, Bowie S, Qiu P, Waller EK, Alexeev A, Sulchek T, Mater. Today 2018, 21, 703.

[33]. Uvizl A, Goswami R, Gandhi SD, Augsburg M, Buchholz F, Guck J, Mansfeld J, Girardo S, Lab on a Chip 2021, 21, 2437. [PubMed: 33977944]

[34]. Joo B, Hur J, Kim G-B, Yun SG, Chung AJ, ACS Nano 2021, 10.1021/acsnano.0c10473.

[35]. Liu Z, Han X, Zhou Q, Chen R, Fruge S, Jo MC, Ma Y, Li Z, Yokoi K, Qin L, Adv. Biosyst 2017, 1, 1700054. [PubMed: 28890929]

[36]. Li J, Wang B, Juba BM, Vazquez M, Kortum SW, Pierce BS, Pacheco M, Roberts L, Strohbach JW, Jones LH, Hett E, Thorarensen A, Telliez J-B, Sharei A, Bunnage M, Gilbert JB, ACS Chem. Biol 2017, 12, 2970. [PubMed: 29088528]

[37]. Matsumoto D, Yamagishi A, Saito M, Sathuluri RR, Silberberg YR, Iwata F, Kobayashi T, Nakamura C, J. Biosci. Bioeng 2016, 122, 748. [PubMed: 27316458]

[38]. Kollmannsperger A, Sharei A, Raulf A, Heilemann M, Langer R, Jensen KF, Wieneke R, Tampé R, Nat. Commun 2016, 7, 10372. [PubMed: 26822409]

[39]. Sharei A, Poceviciute R, Jackson EL, Cho N, Mao S, Hartoularos GC, Jang DY, Jhunjhunwala S, Eyerman A, Schoettle T, Langer R, Jensen KF, Integr. Biol 2014, 6, 470.

[40]. Sharei A, Zoldan J, Adamo A, Sim WY, Cho N, Jackson E, Mao S, Schneider S, Han M-J, Lytton-Jean A, Basto PA, Jhunjhunwala S, Lee J, Heller DA, Kang JW, Hartoularos GC, Kim K-S, Anderson DG, Langer R, Jensen KF, Proc. Natl. Acad. Sci 2013, 110, 2082. [PubMed: 23341631]

[41]. Rong N, Zhou H, Liu R, Wang Y, Fan Z, J. Controlled Release 2018, 273, 40.

[42]. Burgess MT, Porter TM, Ultrasound Med. Biol 2019, 45, 846. [PubMed: 30638968]

[43]. Bhutto DF, Murphy EM, Priddy MC, Centner CC, Moore Iv JB, Bolli R, Kopechek JA, Ultrasound Med. Biol 2018, 44, 2662. [PubMed: 30274682]

[44]. Mahara A, Kobayashi N, Hirano Y, Yamaoka T, Polym. J 2019, 51, 685.

[45]. Belling JN, Heidenreich LK, Tian Z, Mendoza AM, Chiou T-T, Gong Y, Chen NY, Young TD, Wattanatorn N, Park JH, Scarabelli L, Chiang N, Takahashi J, Young SG, Stieg AZ, De Oliveira S, Huang TJ, Weiss PS, Jonas SJ, Proc. Natl. Acad. Sci 2020, 117, 10976. [PubMed: 32358194]

[46]. Karki A, Giddings E, Carreras A, Champagne D, Fortner K, Rincon M, Wu J, Ultrasound Med. Biol 2019, 45, 3222. [PubMed: 31540758]

[47]. Ilovitsh T, Feng Y, Foiret J, Kheirolomoom A, Zhang H, Ingham ES, Ilovitsh A, Tumbale SK, Fite BZ, Wu B, Raie MN, Zhang N, Kare AJ, Chavez M, Qi LS, Pelled G, Gazit D, Vermesh O, Steinberg I, Gambhir SS, Ferrara KW, Proc. Natl. Acad. Sci 2020, 117, 12674. [PubMed: 32430322]

[48]. Lentacker I, Geers B, Demeester J, De Smedt SC, Sanders NN, Mol. Ther 2010, 18, 101. [PubMed: 19623162]

[49]. Fechheimer M, Denny C, Murphy RF, Taylor DL, Eur. J. Cell Biol 1986, 40, 242. [PubMed: 3709548]

[50]. Fechheimer M, Boylan JF, Parker S, Sisken JE, Patel GL, Zimmer SG, Proc. Natl. Acad. Sci 1987, 84, 8463. [PubMed: 2446324]

[51]. Fechheimer M, Taylor DL, in Methods in Cell Biology, Vol. 28 (Ed: Spudich JA), Academic Press 1987, Ch. 9. [PubMed: 3298997]

[52]. Saad AH, Hahn GM, Cancer Res. 1989, 49, 5931. [PubMed: 2790808]

[53]. Fraley R, Subramani S, Berg P, Papahadjopoulos D, J. Biol. Chem 1980, 255, 10431. [PubMed: 6253474]

[54]. Tai-Kin W, Nicolau C, Hofschneider PH, Gene 1980, 10, 87. [PubMed: 6248423]

[55]. Neumann E, Schaefer-Ridder M, Wang Y, Hofschneider PH, The EMBO journal 1982, 1, 841. [PubMed: 6329708]

[56]. Potter H, Weir L, Leder P, Proc. Natl. Acad. Sci 1984, 81, 7161. [PubMed: 6438633]

[57]. Felgner PL, Gadek TR, Holm M, Roman R, Chan HW, Wenz M, Northrop JP, Ringold GM, Danielsen M, Proc. Natl. Acad. Sci 1987, 84, 7413. [PubMed: 2823261]

[58]. Klein TM, Wolf ED, Wu R, Sanford JC, Nature 1987, 327, 70.

[59]. Miller DL, Bao S, Morris JE, Ultrasound Med. Biol 1999, 25, 143. [PubMed: 10048811]

[60]. Ross JP, Cai X, Chiu J-F, Yang J, Wu J, J. Acoust. Soc. Am 2002, 111, 1161. [PubMed: 11931292]

[61]. Lentacker I, De Cock I, Deckers R, De Smedt SC, Moonen CTW, Adv. Drug Delivery Rev 2014, 72, 49.

[62]. Yu J, Chen Z, Yan F, Prog. Biophys. Mol. Biol 2019, 142, 1. [PubMed: 30031881]

[63]. Klibanov AL, Invest. Radiol 2006, 41, 354. [PubMed: 16481920]

[64]. Sboros V, Adv. Drug Delivery Rev 2008, 60, 1117.

[65]. Klibanov AL, Med. Biol. Eng. Comput 2009, 47, 875. [PubMed: 19517153]

[66]. Paefgen V, Doleschel D, Kiessling F, Front. Pharmacol 2015, 6, 197. [PubMed: 26441654]

[67]. Lee H, Kim H, Han H, Lee M, Lee S, Yoo H, Chang JH, Kim H, Biomed. Eng. Lett 2017, 7, 59. [PubMed: 30603152]

[68]. Frinking P, Segers T, Luan Y, Tranquart F, Ultrasound Med. Biol 2020, 46, 892. [PubMed: 31941587]

[69]. Sundaram J, Mellein BR, Mitragotri S, Biophys. J 2003, 84, 3087. [PubMed: 12719239]

[70]. Krasovitski B, Frenkel V, Shoham S, Kimmel E, Proc. Natl. Acad. Sci 2011, 108, 3258. [PubMed: 21300891]

[71]. Zupanc M, Pandur Ž, Stepišnik Perdih T, Stopar D, Petkovšek M, Dular M, Ultrason. Sonochem 2019, 57, 147. [PubMed: 31208610]

[72]. Liu Y, Yan J, Prausnitz MR, Ultrasound Med. Biol 2012, 38, 876. [PubMed: 22425381]

[73]. Miller DL, Thomas RM, Ultrasound Med. Biol 1996, 22, 681. [PubMed: 8865563]

[74]. Mehrdad A, Caroline H, Zeeshan A, Mohan E, Eleanor S, Curr. Pharm. Des 2012, 18, 2118. [PubMed: 22352768]

[75]. Wrenn SP, Dicker SM, Small EF, Dan NR, Mleczko M, Schmitz G, Lewin PA, Theranostics 2012, 2, 1140. [PubMed: 23382772]

[76]. Delalande A, Kotopoulis S, Postema M, Midoux P, Pichon C, Gene 2013, 525, 191. [PubMed: 23566843]

[77]. Panje CM, Wang DS, Willmann JK, Invest. Radiol 2013, 48.

[78]. Wang TY, Wilson KE, Machtaler S, Willmann JK, Curr. Pharm. Biotechnol 2013, 14, 743. [PubMed: 24372231]

[79]. Fan Z, Kumon RE, Deng CX, Ther. Deliv 2014, 5, 467. [PubMed: 24856171]

[80]. Kooiman K, Vos HJ, Versluis M, de Jong N, Adv. Drug Delivery Rev 2014, 72, 28.

[81]. Maresca D, Lakshmanan A, Abedi M, Bar-Zion A, Farhadi A, Lu GJ, Szablowski JO, Wu D, Yoo S, Shapiro MG, Annu. Rev. Chem. Biomol. Eng 2018, 9, 229. [PubMed: 29579400]

[82]. Escoffre J-M, Bouakaz A, Langmuir 2019, 35, 10151. [PubMed: 30525655]

[83]. Chowdhury SM, Abou-Elkacem L, Lee T, Dahl J, Lutz AM, J. Controlled Release 2020, 326, 75.

[84]. Kooiman K, Roovers S, Langeveld SAG, Kleven RT, Dewitte H, O'Reilly MA, Escoffre J-M, Bouakaz A, Verweij MD, Hynynen K, Lentacker I, Stride E, Holland CK, Ultrasound Med. Biol 2020, 46, 1296. [PubMed: 32165014]

[85]. Yang Y, Li Q, Guo X, Tu J, Zhang D, Ultrason. Sonochem 2020, 67, 105096. [PubMed: 32278246]

[86]. Deprez J, Lajoinie G, Engelen Y, De Smedt SC, Lentacker I, Adv. Drug Delivery Rev 2021, 172, 9.

[87]. Li Y, Chen Z, Ge S, BIO Integr. 2021, 2, 29.

[88]. Bouakaz A, Zeghimi A, Doinikov AA, in Therapeutic Ultrasound, Vol. 880 (Eds: Escoffre J-M, Bouakaz A), Springer International Publishing, Cham 2016, Ch. 10.

[89]. Atchley AA, Frizzell LA, Apfel RE, Holland CK, Madanshetty S, Roy RA, Ultrasonics 1988, 26, 280. [PubMed: 3407017]

[90]. Holland CK, Apfel RE, J. Acoust. Soc. Am 1990, 88, 2059. [PubMed: 2269722]

[91]. Apfel RE, Holland CK, Ultrasound Med. Biol 1991, 17, 179. [PubMed: 2053214]

[92]. Chomas JE, Dayton P, May D, Ferrara K, J. Biomed. Opt 2001, 6, 141. [PubMed: 11375723]

[93]. Blake JR, Blake JR, Keen GS, Tong RP, Wilson M, Philos. Trans. R. Soc., A 1999, 357, 251.

[94]. Ohl C-D, Arora M, Ikink R, de Jong N, Versluis M, Delius M, Lohse D, Biophys. J 2006, 91, 4285. [PubMed: 16950843]

[95]. King DA, Malloy MJ, Roberts AC, Haak A, Yoder CC, O'Brien WD Jr., J. Acoust. Soc. Am 2010, 127, 3449. [PubMed: 20550244]

[96]. Sponer J, Czech. J. Phys 1990, 40, 1123.

[97]. Brabec K, Mornstein V, Cent. Eur. J. Biol 2007, 2, 213.

[98]. Jiménez-Fernández J, Crespo A, Ultrasonics 2005, 43, 643. [PubMed: 15890380]

[99]. Rezk AR, Ahmed H, Brain TL, Castro JO, Tan MK, Langley J, Cox N, Mondal J, Li W, Ashokkumar M, Yeo LY, J. Phys. Chem. Lett 2020, 11, 4655. [PubMed: 32453583]

[100]. Rezk AR, Ahmed H, Ramesan S, Yeo LY, Adv. Sci 2021, 8, 2001983.

[101]. Kodama T, Takayama K, Ultrasound Med. Biol 1998, 24, 723. [PubMed: 9695276]

[102]. Helfield BL, Chen X, Qin B, Watkins SC, Villanueva FS, Ultrasound Med. Biol 2017, 43, 2678. [PubMed: 28847500]

[103]. Postema M, van Wamel A, Lancée CT, de Jong N, Ultrasound Med. Biol 2004, 30, 827. [PubMed: 15219962]

[104]. Suslick KS, Eddingsaas NC, Flannigan DJ, Hopkins SD, Xu H, Ultrason. Sonochem 2011, 18, 842. [PubMed: 21247788]

[105]. Juffermans LJM, Dijkmans PA, Musters RJP, Visser CA, Kamp O, Am. J. Physiol. Heart Circ. Physiol 2006, 291, H1595. [PubMed: 16632548]

[106]. Escoffre J-M, Campomanes P, Tarek M, Bouakaz A, Ultrason. Sonochem 2020, 64, 104998. [PubMed: 32062534]

[107]. Wei T, Gu L, Zhou M, Zhou Y, Yang H, Li M, J. Phys. Chem. B 2021, 10.1021/acs.jpcb.1c02483.

[108]. Marmottant P, Hilgenfeldt S, Nature 2003, 423, 153. [PubMed: 12736680]

[109]. Forbes MM, Steinberg RL, O'Brien WD, Ultrasound Med. Biol 2008, 34, 2009. [PubMed: 18692296]

[110]. Collis J, Manasseh R, Liovic P, Tho P, Ooi A, Petkovic-Duran K, Zhu Y, Ultrasonics 2010, 50, 273. [PubMed: 19896683]

[111]. Qiu Y, Zhang C, Tu J, Zhang D, J. Biomech 2012, 45, 1339. [PubMed: 22498312]

[112]. Chettab K, Mestas J-L, Lafond M, Saadna DE, Lafon C, Dumontet C, Mol. Pharm 2017, 14, 441. [PubMed: 28107023]

[113]. Wu J, Ultrasound Med. Biol 2002, 28, 125. [PubMed: 11879959]

[114]. Nejad SM, Hosseini H, Akiyama H, Tachibana K, Theranostics 2016, 6, 446. [PubMed: 26941839]

[115]. Meng L, Liu X, Wang Y, Zhang W, Zhou W, Cai F, Li F, Wu J, Xu L, Niu L, Zheng H, Adv. Sci 2019, 6, 1900557.

[116]. Rong N, Zhang M, Wang Y, Wu H, Qi H, Fu X, Li D, Yang C, Wang Y, Fan Z, Ultrason. Sonochem 2020, 67, 105125. [PubMed: 32298974]

[117]. Qin P, Yutong L, Jin L, Du L, Yu ACH, presented at 2015 IEEE International Ultrasonics Symposium (IUS), Oct., 2015.

[118]. Wang M, Zhang Y, Cai C, Tu J, Guo X, Zhang D, Sci. Rep 2018, 8, 3885. [PubMed: 29497082]

[119]. Yu H, Chen S, Bio-Med. Mater. Eng 2014, 24, 861.

[120]. Qin P, Xu L, Han T, Du L, Yu ACH, Ultrason. Sonochem 2016, 31, 107. [PubMed: 26964929]

[121]. Church CC, Yang X, AIP Conf. Proc 2006, 838, 217.

[122]. van Wamel A, Kooiman K, Harteveld M, Emmer M, ten Cate FJ, Versluis M, de Jong N, J. Controlled Release 2006, 112, 149.

[123]. Duan X, Zhou Q, Wan JMF, Yu ACH, Sci. Rep 2021, 11, 5161. [PubMed: 33664315]

[124]. Delalande A, Kotopoulis S, Rovers T, Pichon C, Postema M, Bubble Sci., Eng., Technol 2011, 3, 3.

[125]. Bjerknes V, Fields of Force, Columbia University Press, New York 1906.

[126]. Huang Y, Das PK, Bhethanabotla VR, Sens. Actuators, Rep 2021, 3, 100041.

[127]. Yosioka K, Kawasima Y, Acta Acustica united with Acustica 1955, 5, 167.
[128]. Kokhuis TJA, Garbin V, Kooiman K, Naaijkens BA, Juffermans LJM, Kamp O, van der Steen AFW, Versluis M, de Jong N, Ultrasound Med. Biol 2013, 39, 490. [PubMed: 23347643]
[129]. Garbin V, Overvelde M, Dollet B, de Jong N, Lohse D, Versluis M, Phys. Med. Biol 2011, 56, 6161. [PubMed: 21878709]
[130]. Postema M, Marmottant P, Lancée CT, Hilgenfeldt S, Jong N. d., Ultrasound Med. Biol 2004, 30, 1337. [PubMed: 15582233]
[131]. Centner CS, Murphy EM, Priddy MC, Moore JT, Janis BR, Menze MA, DeFilippis AP, Kopechek JA, Biomicrofluidics 2020, 14, 024114. [PubMed: 32341725]
[132]. Meng L, Cai F, Jiang P, Deng Z, Li F, Niu L, Chen Y, Wu J, Zheng H, Appl. Phys. Lett 2014, 104, 073701.
[133]. Barnkob R, Augustsson P, Laurell T, Bruus H, Phys. Rev. E 2012, 86, 056307.
[134]. Sadhal SS, Lab on a Chip 2012, 12, 2292. [PubMed: 22660643]
[135]. Wiklund M, Green R, Ohlin M, Lab on a Chip 2012, 12, 2438. [PubMed: 22688253]
[136]. Ahmed D, Ozcelik A, Bojanala N, Nama N, Upadhyay A, Chen Y, Hanna-Rose W, Huang TJ, Nat. Commun 2016, 7, 11085. [PubMed: 27004764]
[137]. Liu S, Yang Y, Ni Z, Guo X, Luo L, Tu J, Zhang D, Zhang Jie, Sensors 2017, 17, 1664.
[138]. Wu M, Ozcelik A, Rufo J, Wang Z, Fang R, Jun Huang T, Microsyst. Nanoeng 2019, 5, 32. [PubMed: 31231539]
[139]. Meng L, Cai F, Li F, Zhou W, Niu L, Zheng H, J. Phys. D: Appl. Phys 2019, 52, 273001.
[140]. Baudoin M, Thomas JL, Annu. Rev. Fluid Mech 2020, 52, 205.
[141]. Zhang P, Bachman H, Ozcelik A, Huang TJ, Annu. Rev. Anal. Chem 2020, 13, 17.
[142]. Bruus H, Lab on a Chip 2012, 12, 1014. [PubMed: 22349937]
[143]. Zarnitsyn VG, Meacham JM, Varady MJ, Hao C, Degertekin FL, Fedorov AG, Biomed. Microdevices 2008, 10, 299. [PubMed: 17994280]
[144]. Carugo D, Ankrett DN, Glynne-Jones P, Capretto L, Boltryk RJ, Zhang X, Townsend PA, Hill M, Biomicrofluidics 2011, 5, 44108. [PubMed: 22662060]
[145]. Rodamporn S, Harris NR, Beeby SP, Boltryk RJ, Sanchez-Eisner T, IEEE Trans. Biomed. Eng 2011, 58, 927. [PubMed: 20977982]
[146]. Friend J, Yeo LY, Reviews of Modern Physics 2011, 83, 647.
[147]. Gedge M, Hill M, Lab on a Chip 2012, 12, 2998. [PubMed: 22842855]
[148]. Salari A, Appak-Baskoy S, Coe IR, Abousawan J, Antonescu CN, Tsai SSH, Kolios MC, Lab on a Chip 2021, 21, 1788. [PubMed: 33734246]
[149]. Ramesan S, Rezk AR, Dekiwadia C, Cortez-Jugo C, Yeo LY, Nanoscale 2018, 10, 13165. [PubMed: 29964280]
[150]. Agostini M, Cecchini M, Nanotechnology 2021, 32, 312001.
[151]. Zhang P, Rufo J, Chen C, Xia J, Tian Z, Zhang L, Hao N, Zhong Z, Gu Y, Chakrabarty K, Huang TJ, Nat. Commun 2021, 12, 3844. [PubMed: 34158489]
[152]. Ding X, Li P, Lin S-CS, Stratton ZS, Nama N, Guo F, Slotcavage D, Mao X, Shi J, Costanzo F, Huang TJ, Lab on a Chip 2013, 13, 3626. [PubMed: 23900527]
[153]. Yeo LY, Friend JR, Annu. Rev. Fluid Mech 2014, 46, 379.
[154]. Ozcelik A, Rufo J, Guo F, Gu Y, Li P, Lata J, Huang TJ, Nat. Methods 2018, 15, 1021. [PubMed: 30478321]
[155]. Gao Y, Fajrial AK, Yang T, Ding X, Biomater. Sci 2021, 9, 1574. [PubMed: 33283794]
[156]. Destgeer G, Sung HJ, Lab on a Chip 2015, 15, 2722. [PubMed: 26016538]
[157]. Go DB, Atashbar MZ, Ramshani Z, Chang H-C, Anal. Methods 2017, 9, 4112. [PubMed: 29151901]
[158]. Boluriaan S, Morris PJ, Int. J. Aeroacoust 2003, 2, 255.
[159]. Huang P-H, Xie Y, Ahmed D, Rufo J, Nama N, Chen Y, Chan CY, Huang TJ, Lab on a Chip 2013, 13, 3847. [PubMed: 23896797]

[160]. Huang P-H, Nama N, Mao Z, Li P, Rufo J, Chen Y, Xie Y, Wei C-H, Wang L, Huang TJ, Lab on a Chip 2014, 14, 4319. [PubMed: 25188786]

[161]. Nama N, Huang TJ, Costanzo F, J. Fluid Mech 2017, 825, 600. [PubMed: 29051631]

[162]. Doinikov AA, Gerlt MS, Pavlic A, Dual J, Microfluid. Nanofluid 2020, 24, 32.

[163]. Zhu H, Zhang P, Zhong Z, Xia J, Rich J, Mai J, Su X, Tian Z, Bachman H, Rufo J, Gu Y, Kang P, Chakrabarty K, Witelski TP, Huang TJ, Sci. Adv 2021, 7, eabc7885. [PubMed: 33523965]

[164]. Zhang SP, Lata J, Chen C, Mai J, Guo F, Tian Z, Ren L, Mao Z, Huang P-H, Li P, Yang S, Huang TJ, Nat. Commun 2018, 9, 2928. [PubMed: 30050088]

[165]. Zhang P, Chen C, Su X, Mai J, Gu Y, Tian Z, Zhu H, Zhong Z, Fu H, Yang S, Chakrabarty K, Huang TJ, Sci. Adv 2020, 6, eaba0606. [PubMed: 32577516]

[166]. Wu J, Ross JP, Chiu J-F, J. Acoust. Soc. Am 2002, 111, 1460. [PubMed: 11931323]

[167]. Thein M, Cheng A, Khanna P, Zhang C, Park E-J, Ahmed D, Goodrich CJ, Asphahani F, Wu F, Smith NB, Dong C, Jiang X, Zhang M, Xu J, Biosens. Bioelectron 2011, 27, 25. [PubMed: 21783355]

[168]. Sangpil Y, Yingxiao W, Shung KK, presented at SPIE BIOS, Apr., 2016.

[169]. Yoon S, Kim MG, Chiu CT, Hwang JY, Kim HH, Wang Y, Shung KK, Sci. Rep 2016, 6, 20477. [PubMed: 26843283]

[170]. Yoon S, Wang P, Peng Q, Wang Y, Shung KK, Sci. Rep 2017, 7, 5275. [PubMed: 28706248]

[171]. Kim MG, Yoon S, Chiu CT, Shung KK, Ultrasound Med. Biol 2018, 44, 622. [PubMed: 29284555]

[172]. Kim S, Moon S, Rho S, Yoon S, Appl. Phys. Lett 2021, 118, 184102. [PubMed: 33981116]

[173]. Zhang Z, Wang Y, Zhang H, Tang Z, Liu W, Lu Y, Wang Z, Yang H, Pang W, Zhang H, Zhang D, Duan X, Small 2017, 13, 1602962.

[174]. Lu Y, del Vries WC, Overeem NJ, Duan X, Zhang H, Zhang H, Pang W, Ravoo BJ, Huskens J, Angew. Chem. Int. Ed 2019, 58, 159.

[175]. Lu Y, Huskens J, Pang W, Duan X, Mater. Chem. Front 2019, 3, 782.

[176]. Lu Y, Palanikumar L, Choi ES, Huskens J, Ryu J-H, Wang Y, Pang W, Duan X, ACS Appl. Mater. Interfaces 2019, 11, 19734. [PubMed: 31090387]

[177]. Pan S, Jeon T, Luther DC, Duan X, Rotello VM, ACS Appl. Mater. Interfaces 2020, 12, 15823. [PubMed: 32150373]

[178]. Guo X, Sun M, Yang Y, Xu H, Liu J, He S, Wang Y, Xu L, Pang W, Duan X, Adv. Sci 2021, 8, 2002489.

[179]. Ramesan S, Rezk AR, Cevaal PM, Cortez-Jugo C, Symons J, Yeo LY, ACS Appl. Bio Mater 2021, 4, 2781.

[180]. Kamenac A, Schilberth FL, Wagner E, Wixforth A, Lächelt U, Westerhausen C, Processes 2021, 9.

[181]. Dewey WC, Hopwood LE, Sapareto SA, Gerweck LE, Radiology 1977, 123, 463. [PubMed: 322205]

[182]. Sapareto SA, Hopwood LE, Dewey WC, Raju MR, Gray JW, Cancer Res. 1978, 38, 393. [PubMed: 563767]

[183]. Roti Roti JL, Int. J. Hyperthermia 2008, 24, 3. [PubMed: 18214765]

[184]. Papahadjopoulos D, Jacobson K, Nir S, Isac I, Biochim. Biophys. Acta 1973, 311, 330. [PubMed: 4729825]

[185]. Blicher A, Wodzinska K, Fidorra M, Winterhalter M, Heimburg T, Biophys. J 2009, 96, 4581. [PubMed: 19486680]

[186]. Yamashita Y-I, Shimada M, Tachibana K, Harimoto N, Tsujita E, Shirabe K, Miyazaki J-I, Sugimachi K, Hum. Gene Ther 2002, 13, 2079. [PubMed: 12490002]

[187]. Escoffre JM, Kaddur K, Rols MP, Bouakaz A, Ultrasound Med. Biol 2010, 36, 1746. [PubMed: 20850028]

[188]. Longsine-Parker W, Wang H, Koo C, Kim J, Kim B, Jayaraman A, Han A, Lab on a Chip 2013, 13, 2144. [PubMed: 23615834]

[189]. Meacham JM, Durvasula K, Degertekin FL, Fedorov AG, Sci. Rep 2018, 8, 3727. [PubMed: 29487375]

[190]. Hsi P, Christianson RJ, Dubay RA, Lissandrello CA, Fiering J, Balestrini JL, Tandon V, Lab on a Chip 2019, 19, 2978. [PubMed: 31410419]

[191]. Lee YH, Peng CA, Gene Ther. 2005, 12, 625. [PubMed: 15647763]

[192]. Aghaamoo M, Chen Y-H, Li X, Garg N, Jiang R, Lee AP, bioRxiv 2021, 10.1101/2021.02.16.4315462021.02.16.431546.

[193]. Denais CM, Gilbert RM, Isermann P, McGregor AL, te Lindert M, Weigelin B, Davidson PM, Friedl P, Wolf K, Lammerding J, Science 2016, 352, 353. [PubMed: 27013428]

[194]. Isermann P, Lammerding J, Nucleus 2017, 8, 268. [PubMed: 28287898]

[195]. Shah P, Hobson CM, Cheng S, Colville MJ, Paszek MJ, Superfine R, Lammerding J, Curr. Biol 2021, 31, 753. [PubMed: 33326770]

[196]. Salari A, Appak-Baskoy S, Ezzo M, Hinz B, Kolios MC, Tsai SSH, Small 2020, 16, 1903788.

[197]. Seidel W, Hesjedal T, presented at IEEE Symposium on Ultrasonics, 2003, 5-8 Oct. 2003, 2003.

[198]. Li D, Cahill DG, Phys. Rev. B 2016, 94, 104306.

[199]. Wang L, Chen S, Zhang J, Zhou J, Yang C, Chen Y, Duan H, Appl. Phys. Lett 2018, 113, 093503.

[200]. Zheng J, Zhou J, Zeng P, Liu Y, Shen Y, Yao W, Chen Z, Wu J, Xiong S, Chen Y, Shi X, Liu J, Fu Y, Duan H, Appl. Phys. Lett 2020, 116, 123502.

[201]. Cui W, Pang W, Yang Y, Li T, Duan X, Nanotechnol. Precis. Eng 2019, 2, 15.

[202]. Zhang J, Yang S, Chen C, Hartman JH, Huang P-H, Wang L, Tian Z, Zhang P, Faulkenberry D, Meyer JN, Huang TJ, Lab on a Chip 2019, 19, 984. [PubMed: 30768117]

[203]. Zhang J, Hartman JH, Chen C, Yang S, Li Q, Tian Z, Huang P-H, Wang L, Meyer JN, Huang TJ, Lab on a Chip 2020, 20, 1729. [PubMed: 32292982]

[204]. Chen C, Gu Y, Philippe J, Zhang P, Bachman H, Zhang J, Mai J, Rufo J, Rawls JF, Davis EE, Katsanis N, Huang TJ, Nat. Commun 2021, 12, 1118. [PubMed: 33602914]

[205]. Shi J, Ahmed D, Mao X, Lin S-CS, Lawit A, Huang TJ, Lab on a Chip 2009, 9, 2890. [PubMed: 19789740]

[206]. Ding X, Lin S-CS, Kiraly B, Yue H, Li S, Chiang IK, Shi J, Benkovic SJ, Huang TJ, Proc. Natl. Acad. Sci 2012, 109, 11105. [PubMed: 22733731]

[207]. Ding X, Lin S-CS, Lapsley MI, Li S, Guo X, Chan CY, Chiang IK, Wang L, McCoy JP, Huang TJ, Lab on a Chip 2012, 12, 4228. [PubMed: 22992833]

[208]. Ding X, Peng Z, Lin S-CS, Geri M, Li S, Li P, Chen Y, Dao M, Suresh S, Huang TJ, Proc. Natl. Acad. Sci 2014, 111, 12992. [PubMed: 25157150]

[209]. Guo F, Li P, French JB, Mao Z, Zhao H, Li S, Nama N, Fick JR, Benkovic SJ, Huang TJ, Proc. Natl. Acad. Sci 2014, 10.1073/pnas.1422068112201422068.

[210]. Li S, Guo F, Chen Y, Ding X, Li P, Wang L, Cameron CE, Huang TJ, Anal. Chem 2014, 86, 9853. [PubMed: 25232648]

[211]. Guo F, Mao Z, Chen Y, Xie Z, Lata JP, Li P, Ren L, Liu J, Yang J, Dao M, Suresh S, Huang TJ, Proc. Natl. Acad. Sci 2016, 113, 1522. [PubMed: 26811444]

[212]. Kang P, Tian Z, Yang S, Yu W, Zhu H, Bachman H, Zhao S, Zhang P, Wang Z, Zhong R, Huang TJ, Lab on a Chip 2020, 20, 987. [PubMed: 32010910]

[213]. Xie Y, Mao Z, Bachman H, Li P, Zhang P, Ren L, Wu M, Huang TJ, J. Biomech. Eng 2020, 142, 0310051.

[214]. Zhang N, Zuniga-Hertz JP, Zhang EY, Gopesh T, Fannon MJ, Wang J, Wen Y, Patel HH, Friend J, Lab on a Chip 2021, 21, 904. [PubMed: 33438699]

[215]. Lenshof A, Laurell T, Chem. Soc. Rev 2010, 39, 1203. [PubMed: 20179832]

[216]. Inui T, Mei J, Imashiro C, Kurashina Y, Friend J, Takemura K, Lab on a Chip 2021, 21, 1299. [PubMed: 33734243]

[217]. Collins DJ, Morahan B, Garcia-Bustos J, Doerig C, Plebanski M, Neild A, Nat. Commun 2015, 6, 8686. [PubMed: 26522429]

[218]. Collins DJ, Devendran C, Ma Z, Ng JW, Neild A, Ai Y, Sci. Adv 2016, 2, e1600089. [PubMed: 27453940]

[219]. Shi J, Mao X, Ahmed D, Colletti A, Huang TJ, Lab on a Chip 2008, 8, 221. [PubMed: 18231658]

[220]. Shi J, Yazdi S, Steven Lin S-C, Ding X, Chiang IK, Sharp K, Huang TJ, Lab on a Chip 2011, 11, 2319. [PubMed: 21709881]

[221]. Mao Z, Li P, Wu M, Bachman H, Mesyngier N, Guo X, Liu S, Costanzo F, Huang TJ, ACS Nano 2017, 11, 603. [PubMed: 28068078]

[222]. Wu M, Ouyang Y, Wang Z, Zhang R, Huang P-H, Chen C, Li H, Li P, Quinn D, Dao M, Suresh S, Sadovsky Y, Huang TJ, Proc. Natl. Acad. Sci 2017, 114, 10584. [PubMed: 28923936]

[223]. Wu M, Chen C, Wang Z, Bachman H, Ouyang Y, Huang P-H, Sadovsky Y, Huang TJ, Lab on a Chip 2019, 19, 1174. [PubMed: 30806400]

[224]. Shilton R, Tan MK, Yeo LY, Friend JR, J. Appl. Phys 2008, 104, 014910.

[225]. Li H, Friend JR, Yeo LY, Phys. Rev. Lett 2008, 101, 084502. [PubMed: 18764621]

[226]. Li H, Friend JR, Yeo LY, Biomed. Microdevices 2007, 9, 647. [PubMed: 17530412]

[227]. Guo J, Li JLW, Chen Y, Yeo LY, Friend JR, Kang Y, IEEE Trans. Microwave Theory Tech 2014, 62, 1898.

[228]. Collins DJ, O'Rorke R, Neild A, Han J, Ai Y, Soft Matter 2019, 15, 8691. [PubMed: 31657435]

[229]. Behrens J, Langelier S, Rezk AR, Lindner G, Yeo LY, Friend JR, Lab on a Chip 2015, 15, 43. [PubMed: 25343424]

[230]. Liu YJ, Ding X, Lin S-CS, Shi J, Chiang IK, Huang TJ, Adv. Mater 2011, 23, 1656. [PubMed: 21438028]

[231]. Liu YJ, Lu M, Ding X, Leong ESP, Lin S-CS, Shi J, Teng JH, Wang L, Bunning TJ, Huang TJ, J. Lab. Autom 2012, 18, 291. [PubMed: 22909448]

[232]. Guo F, Zhou W, Li P, Mao Z, Yennawar NH, French JB, Huang TJ, Small 2015, 11, 2733. [PubMed: 25641793]

[233]. Ramesan S, Rezk AR, Yeo LY, Lab on a Chip 2018, 18, 3272. [PubMed: 30225496]

[234]. Doinikov AA, Bouakaz A, J. Acoust. Soc. Am 2010, 128, 11. [PubMed: 20649196]

[235]. Forbes MM, O'Brien WD Jr., J. Acoust. Soc. Am 2012, 131, 2723. [PubMed: 22501051]

[236]. Chen C, Gu Y, Tu J, Guo X, Zhang D, Ultrasonics 2016, 66, 54. [PubMed: 26651263]

[237]. Cowley J, McGinty S, Ultrasonics 2019, 96, 214. [PubMed: 30739724]

[238]. Man VH, Truong PM, Li MS, Wang J, Van-Oanh N-T, Derreumaux P, Nguyen PH, J. Phys. Chem. B 2019, 123, 71. [PubMed: 30540473]

[239]. Mobadersany N, Sarkar K, J. Fluid Mech 2019, 875, 781.

[240]. Sojahrood AJ, Haghi H, Li Q, Porter TM, Karshafian R, Kolios MC, Ultrason. Sonochem 2020, 66, 105070. [PubMed: 32279052]

[241]. Muller PB, Bruus H, Phys. Rev. E 2015, 92, 063018.

[242]. Karlsen JT, Qiu W, Augustsson P, Bruus H, Phys. Rev. Lett 2018, 120, 054501. [PubMed: 29481204]

[243]. Qiu W, Karlsen JT, Bruus H, Augustsson P, Phys. Rev. Appl 2019, 11, 024018.

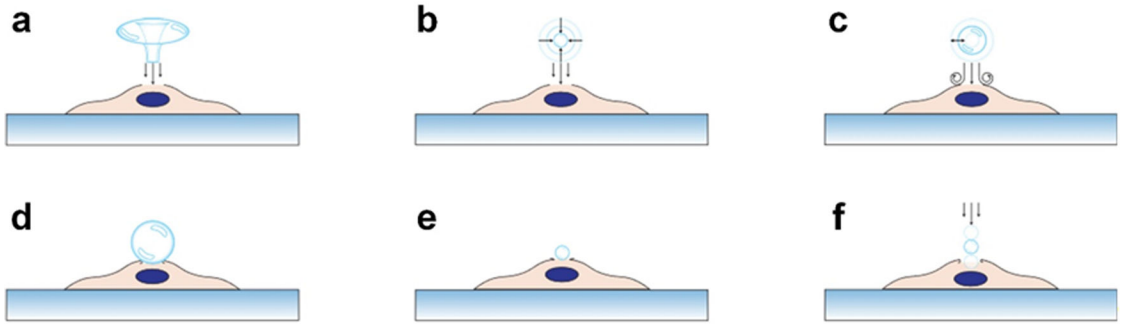

Figure 1.

Schematics for illustrating the bubble-based sonoporation mechanisms. They illustrate mechanisms based on (a) the jetting effect caused by a bubble undergoing inertial cavitation, (b) the shock waves generated from a collapsing bubble, (c) the acoustic streaming induced by a stable oscillating bubble, (d) the pushing effect on the cell membrane induced by bubble expansion during oscillation, (e) the pulling effect on the cell membrane induced by bubble contraction during oscillation, (f) the force applied on the cell membrane by a bubble that is pushed through the membrane under an acoustic radiation force.

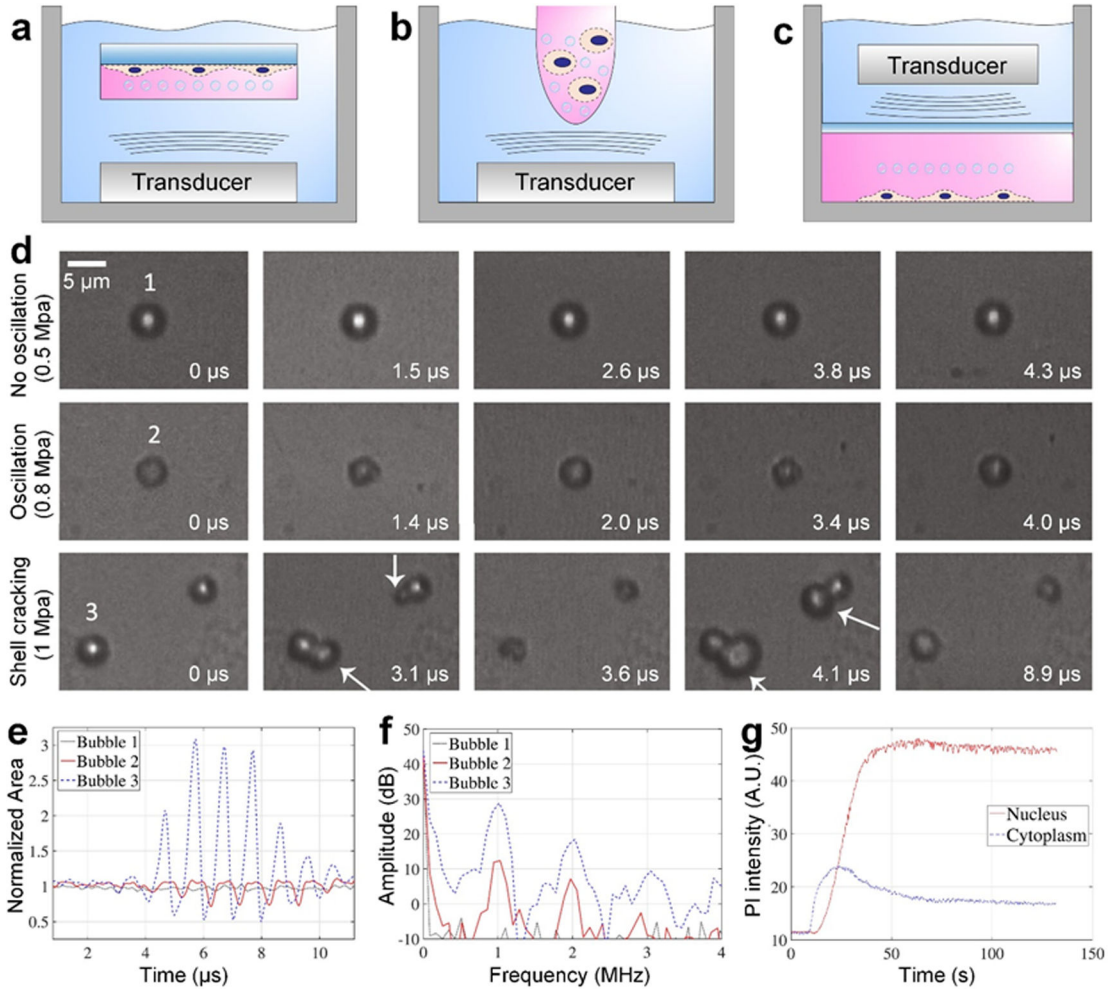

Figure 2.

Conventional bubble-based sonoporation technologies. (a-c) Schematics for illustrating the typical setups, which usually have a sonicating bath and a chamber containing cells and bubbles. (a) The typical setup with an ultrasonic transducer at the bottom of the bath and a chamber (*e.g.*, sealed petri dish) with cells adhered on the chamber wall. (b) The typical setup with an ultrasonic transducer at the bottom of the bath and a chamber (*e.g.*, Eppendorf tube) with cells in suspension. (c) The typical setup having a chamber (*e.g.*, customized sealed chamber) with suspension/adherent cells at the bottom of the bath and an ultrasonic transducer at the top of the bath. The transducers in (a) to (c) can either be planar or focused ultrasonic transducers. (d) Experimental results showing that bubbles in acoustic fields can have different dynamic behaviors, such as limited oscillations with small deformation at the acoustic pressure of 0.5 MPa (top row), asymmetric compression/expansion oscillations at 0.8 MPa (middle row), and acoustic wave-induced shell cracking at 1 MPa (bottom row). White arrows point to the bubbles with gas release induced by shell cracking. (e) The histories of normalized bubble areas for quantitatively characterizing different dynamic behaviors observed in (d). (f) The response frequencies of bubbles showing nonlinear components. (g) Quantitative characterization of sonoporation induced propidium iodide (PI) intensity changes in the cytoplasm and nucleus with respect to time. The experimental

results were acquired using endothelial cells, an acoustic frequency of 2 MHz, and a peak-negative acoustic pressure of 0.9 MPa. (d-g) Reproduced with permission.[102] 2017, Ultrasound in Medicine and Biology.

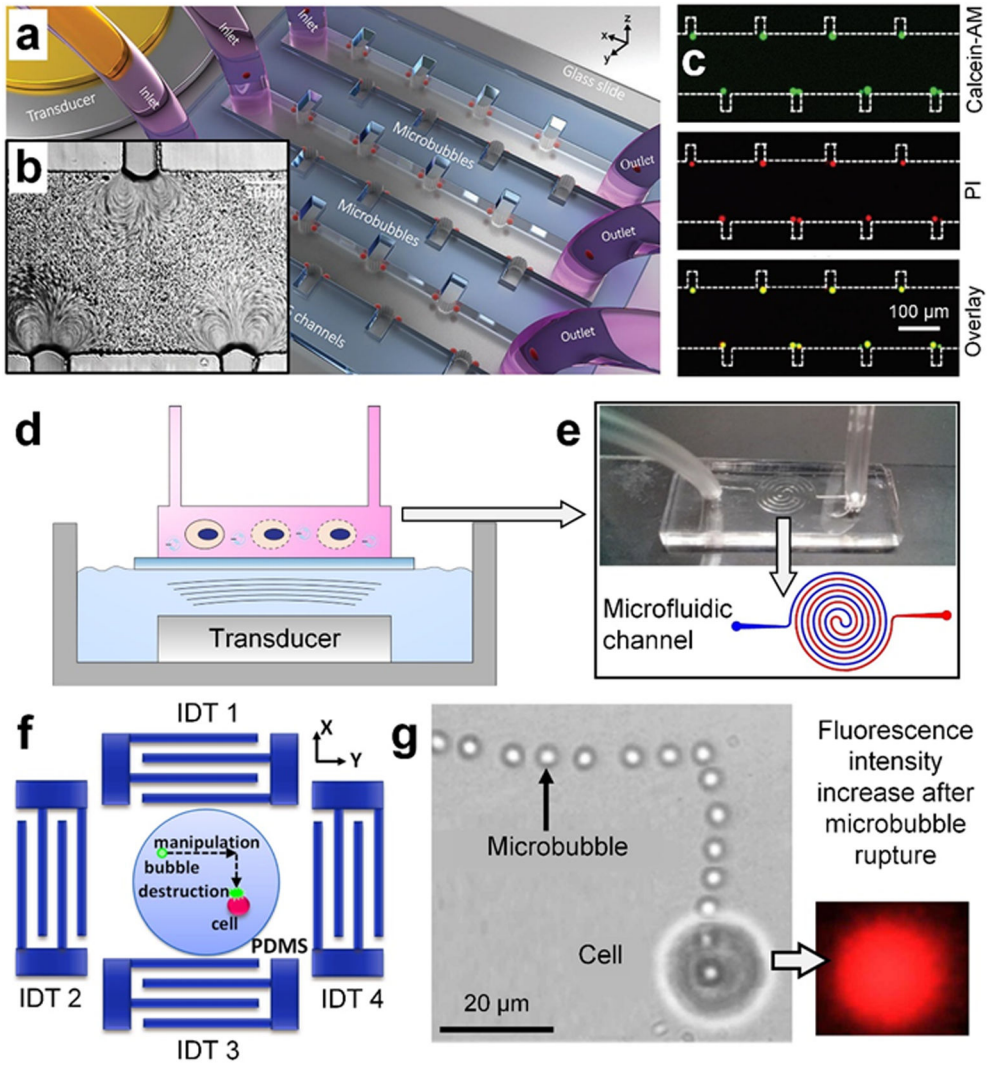

Figure 3.

Recent sonoporation technologies that fuse bubble-based sonoporation and microfluidics. (a) A schematic of a device that can trap an array of microbubbles along the sidewalls of microfluidic channels and apply acoustic waves to induced stable cavitation (*i.e.,* oscillation of trapped bubbles). The bubble oscillation further generates vortex streaming, which can trap cells near the bubble shells and apply shear forces to increase the bubble permeability. (b) A microscopic image showing vortex streaming caused by oscillating bubbles. (c) Sonoporation results of MDA-MB-231 cells by using the bubble-based microfluidic device. Calcein-AM (green) is used to show viability and propidium iodide (PI, red) is used to indicate the membrane permeability change. (a-c) Reproduced with permission.[115] 2019, Advanced Science. (d) A schematic of a setup that fuses the conventional sonicating bath and a microfluidic channel for continuous sonoporation. (e, top and bottom) A photo and a schematic of a spiral microfluidic channel for cells to flow through. The spiral configuration allows for controlling the cell residence time in the microfluidic channel so that cells experience sufficient treatment time. (d-e) Reproduced with permission.[131] 2020, Biomicrofluidics. (f) A schematic of a setup that leverages surface acoustic wave-based

acoustic tweezers to precisely move a microbubble to a target cell and then apply an acoustic pulse to enable inertial bubble cavitation at the cell location for sonoporation. (g, left) A stacked image showing a bubble can be translated following a complex path to a target cell. (g, right) A captured fluorescence image showing that PI (red) can successfully enter the transiently porous cell, after inertial bubble cavitation. (f-g) Reproduced with permission. [132] 2014, Applied Physics Letters.

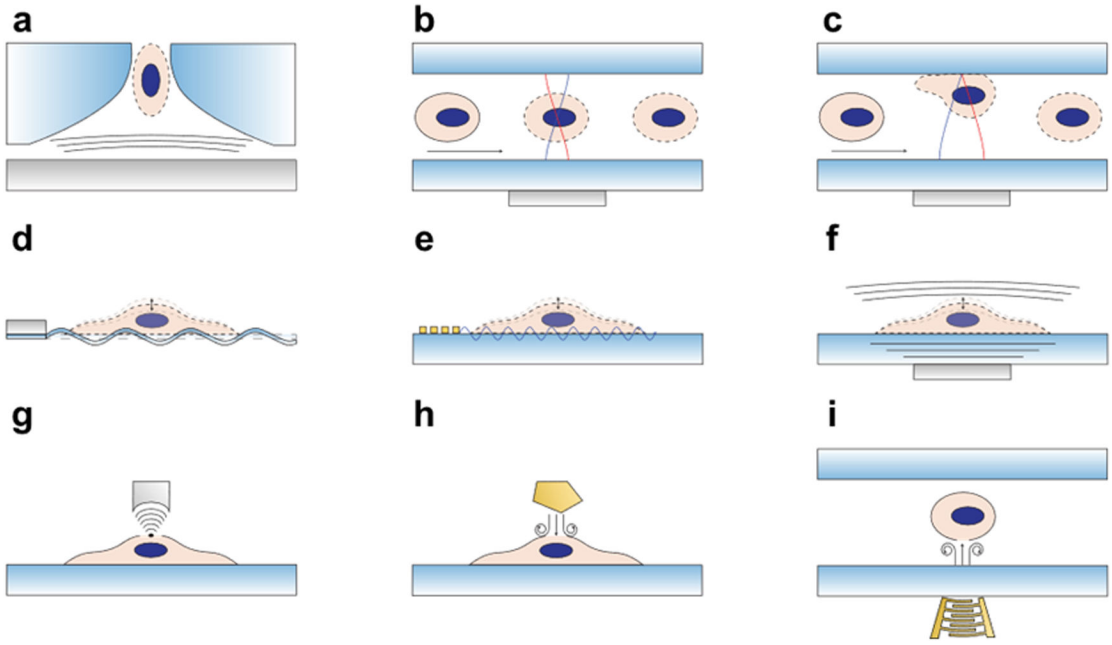

Figure 4.

Schematics for illustrating non-bubble-based sonoporation mechanisms. To increase the membrane permeability, different mechanisms have been used, including (a) using travelling acoustic waves to eject a cell through a nozzle orifice for sonoporation, (b) using standing acoustic waves in a half wavelength resonator to push cells to the center of the resonator for sonoporation of cells flowing through the resonator, (c) using standing acoustic waves in a quarter wavelength resonator (or a thin resonator) to push cells to the wall of the resonator for sonoporation of cells flowing through the resonator, (d) using Lamb waves (or flexural waves) propagating along a thin-wall substrate for sonoporation of cells adhered on the substrate, (e) using surface acoustic waves propagating along the surface of a substrate for sonoporation of cells adhered on the substrate, (f) using travelling bulk acoustic waves for sonoporation of adherent cells in the area above the acoustic transducer, (g) using focused bulk acoustic waves with concentrated energy for localized sonoporation of a single cell adhered on a substrate, (h) using acoustic streaming induced by hyper-frequency bulk acoustic waves for sonoporation of adherent cells in a small area near the wave source, and (i) using acoustic streaming induced by focused surface acoustic waves for sonoporation of cells in a glass well plate.

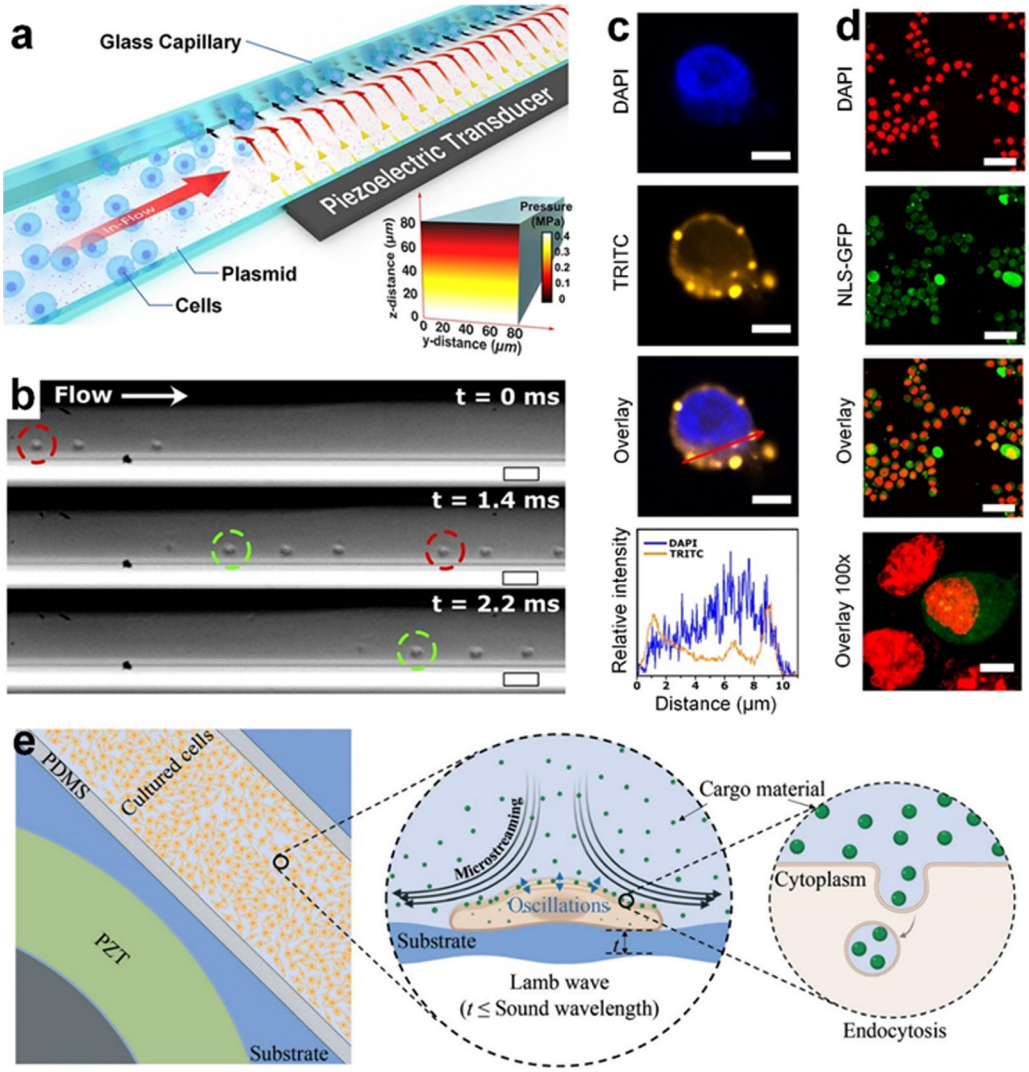

Figure 5.

Sonoporation technologies based on low-frequency bulk acoustic waves and Lamb waves. (a) A schematic of a bulk acoustic wave resonator-based sonoporation device, composed of a glass capillary coated with cargos and a piezoelectric transducer. (b) Microscopic image showing that the acoustic radiation force can push Jurkat cells on the capillary wall coated with cargos, as the cells flow through the capillary. (c) Confocal microscope images showing that Cy3-labeled DNA (TRITC channel, orange) can be delivered to a Jurkat cell. The nucleus is stained with 4,6-diamidino-2-phenylindole (DAPI, blue). (c, bottom) Fluorescence intensity plots showing the distributions of DAPI and TRITC across the cell and indicating that TRITC can be delivered to the nucleus. (d) Confocal images of mouse embryonic fibroblasts that were virally transduced with a nuclear localization signal green fluorescent protein (NLS-GFP), treated with the acoustofluidic device, fixed, and stained with DAPI (red). The NLS-GFP allowed for the observation of perturbations to the cell nuclei. The acquired overlay images indicate nuclear envelope rupture, allowing for the delivery of DNA into the nucleus. (a-d) Reproduced with permission.[45] 2020, Proceedings of the National Academy of Sciences. (e) A Schematic of a Lamb wave-based sonoporation

device that consists of a surface bonded piezoelectric disk, a polydimethylsiloxane (PDMS) chamber, and a glass substrate with adherent cells. The Lamb wave generated by the transducer can propagate along the glass substrate, temporarily permeabilize the cell, and induce microstreaming to enhance both the delivery of cargos to the cell membrane and endocytosis. Reproduced with permission.[148] 2021, Lab on a Chip.

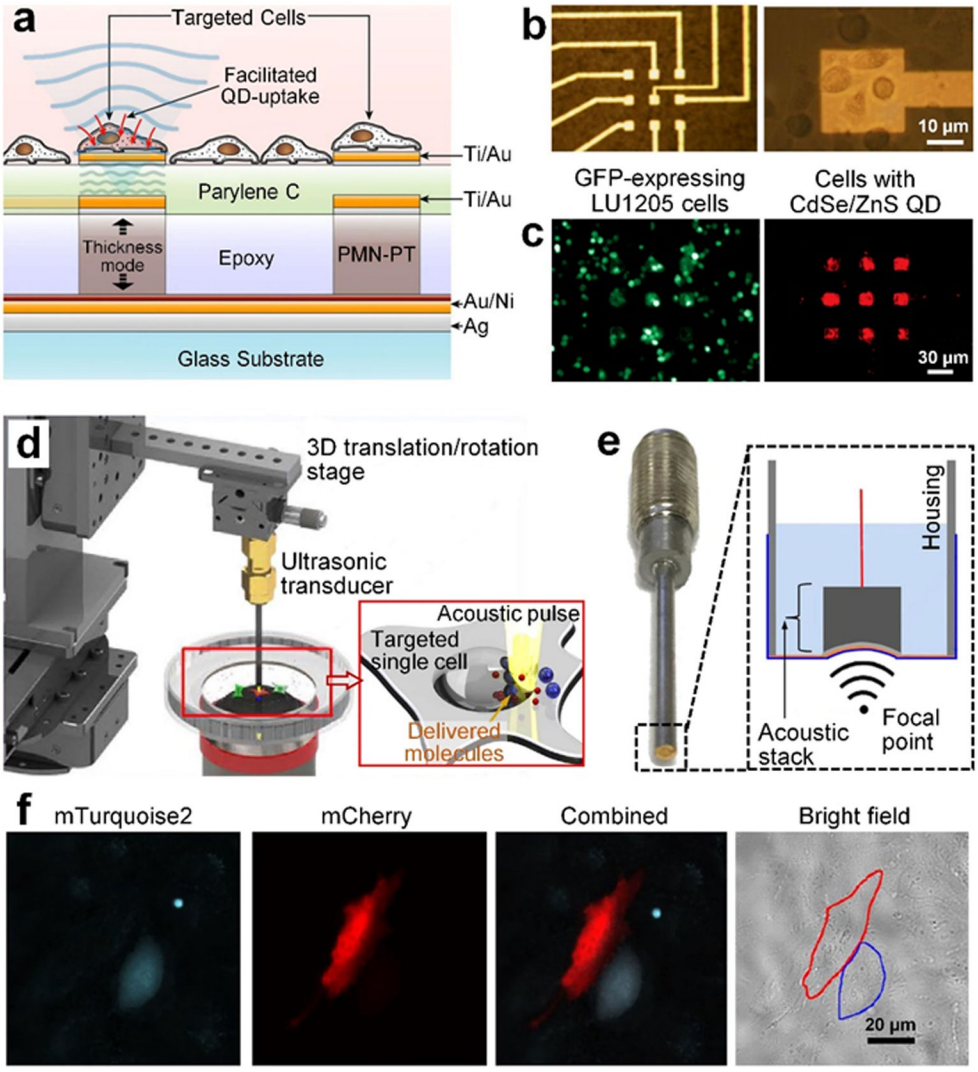

Figure 6.

Sonoporation technologies based on high-frequency bulk acoustic waves. (a) A schematic of a sonoporation device that utilizes lead magnesium niobate-lead titanate (PMN-PT) micropillars to generate high-frequency (~30 MHz) bulk acoustic waves for the sonoporation of cells seeded on gold electrodes above the micropillars. (b) A bright field image of fabricated 3×3 micropillars with gold electrodes as well as cells adhered on the electrodes. (c) Quantum dots (CdSe/ZnS QD) can be successfully delivered to green fluorescent protein (GFP) expressing human melanoma (LU1205) cells seeded above the micropillars. (a-c) Reproduced with permission.[167] 2011, Biosensors and Bioelectronics. (d) A schematic of a platform that uses focused high-frequency (~150 MHz) ultrasonic waves for single-cell sonoporation. By using a stage to precisely control the ultrasonic transducer's position, this platform can be used for the sonoporation of any target cell adhered on the petri dish. (e) An image and a schematic of the ultrasonic transducer, which relies on a curved lithium niobate ($LiNbO_3$) layer to generate focused ultrasonic waves with concentrated energy in a narrow ultrasonic beam. (f) Experimental results showing that two different proteins, mTurquoise2

and mCherry, that can be successfully delivered to two neighboring cells. (d-f) Reproduced with permission.[169-170] 2016, 2017, Scientific Reports.

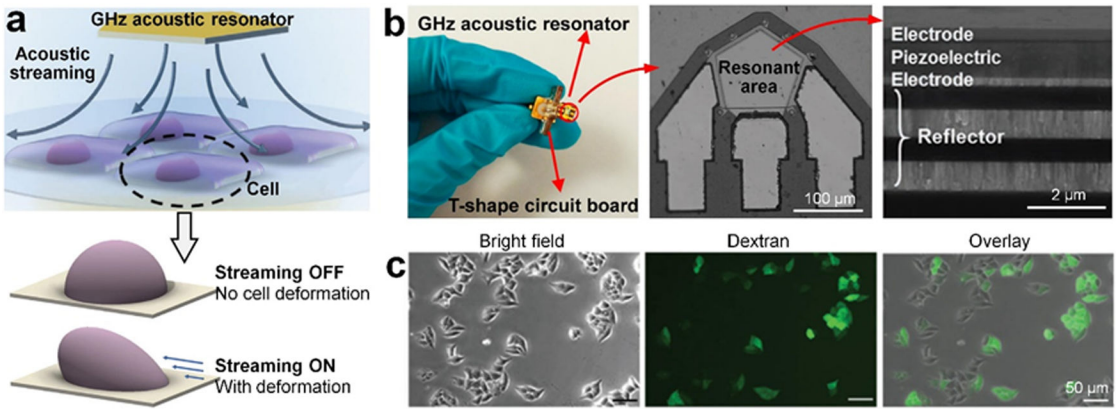

Figure 7.

Sonoporation technology based on acoustic streaming induced by hyper-frequency bulk acoustic waves. (a) A schematic of a setup that uses a pentagon-shaped GHz acoustic resonator to generate hyper-frequency bulk acoustic waves, which further induce acoustic streaming. The acoustic streaming can apply shear forces on cells adhered on a substrate to deform the cell for temporary membrane permeabilization. Reproduced with permission.[178] 2021, Advanced Science. (b, left to right) A photo of a GHz acoustic resonator, a scanning electron microscopy (SEM) image of the resonant area, and a cross-section SEM image of the GHz acoustic resonator. Reproduced with permission.[173, 177] 2020, ACS Applied Materials and Interfaces and 2017, Small. (c) Microscopic images showing HeLa cells with 40 kDa fluorescein isothiocyanate (FITC) dextran after sonoporation using the GHz resonator for 10 min. Reproduced with permission.[178] 2021, Advanced Science.

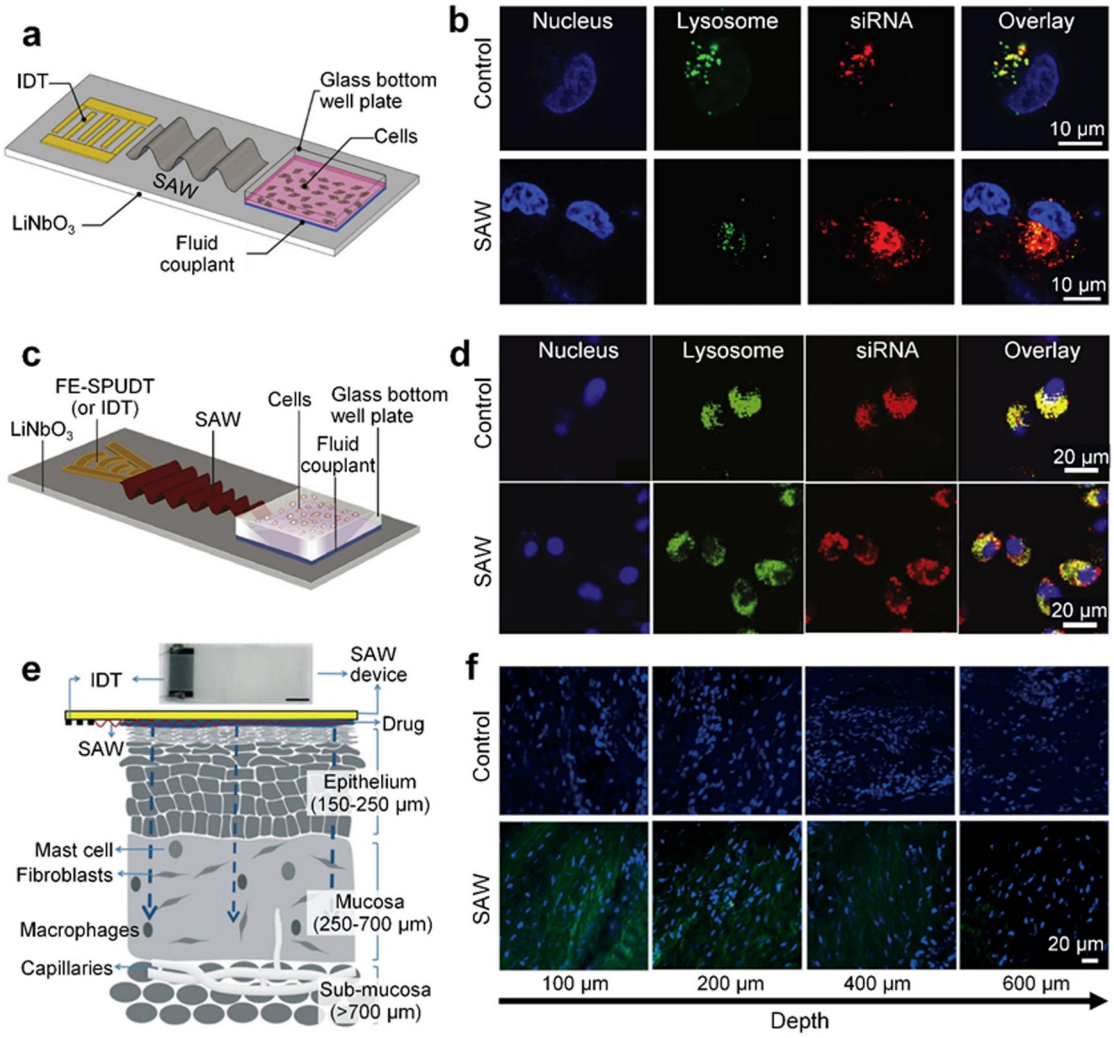

Figure 8.

Surface acoustic wave-based permeabilization technologies. (a) A schematic of a platform that uses a straight interdigital transducer (IDT) on a lithium niobate ($LiNbO_3$) wafer to generate surface acoustic waves (SAWs) for the acoustically-mediated delivery to cells adhered on the glass bottom of a well plate. In this platform, the energy of the surface acoustic waves is coupled to the glass well plate using a fluid couplant. (b) Confocal microscopy images of HeLa cells with and without the surface acoustic wave-based sonoporation. Compared to the group without surface acoustic waves, the siRNA cargos are more efficiently delivered to the cells in the group with surface acoustic waves. (a-b) Reproduced with permission.[149] 2018, Nanoscale. (c) A schematic of a platform that uses a focused elliptical single-phase unidirectional transducer (FE-SPUDT) on a $LiNbO_3$ wafer to generate focused surface acoustic waves for the permeabilization of suspension cells in a glass well plate. (d) Confocal microscopy images of Jurkat cells with and without surface acoustic wave-based sonoporation. For the group treated with surface acoustic waves, the delivered siRNA cargos are found to overlap less with the lysosomes. (c-d) Reproduced with permission.[179] 2021, ACS Applied Bio Materials. (e) A schematic of a setup for the delivery of drug to the mucosal layer by using surface acoustic waves. (f) Microscopy

images showing the distributions of fluorescein isothiocyanate (FITC) albumin (green) in multiple layers of the porcine lip tissue at different depths, after surface acoustic wave-based sonoporation. (e-f) Reproduced with permission.[233] 2018, Lab on a Chip.

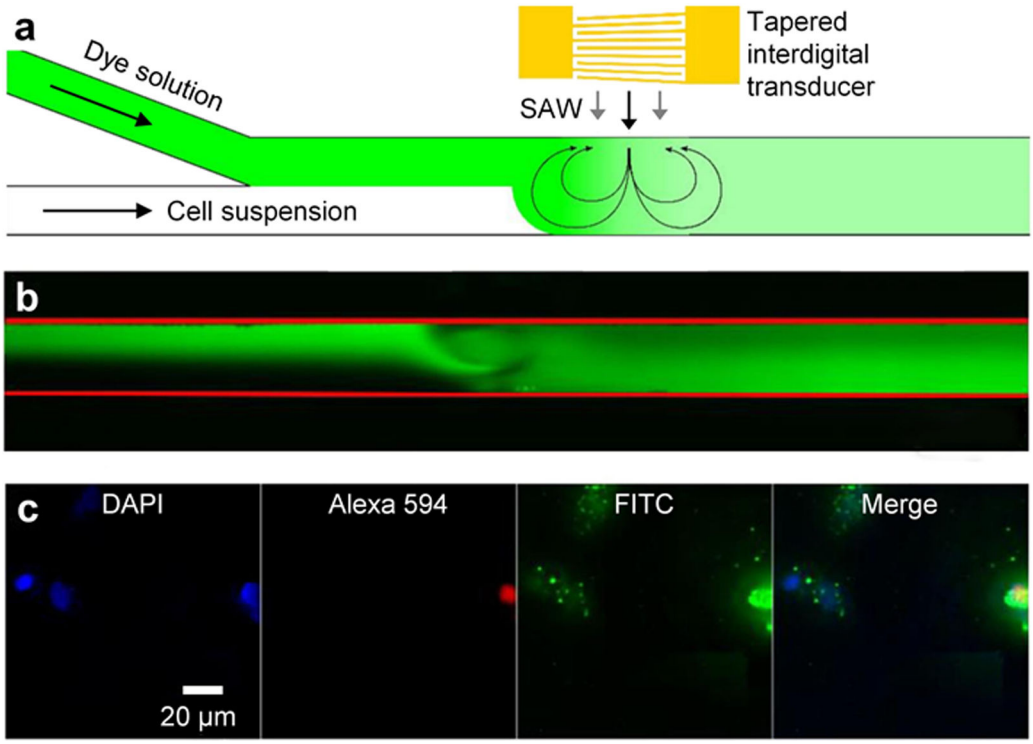

Figure 9.

Sonoporation technology relying on acoustic streaming induced by surface acoustic waves. (a) A schematic of a platform that uses acoustic streaming induced by traveling surface acoustic waves for the sonoporation of cells flowing through a microfluidic channel. (b) An acquired microscopy image showing acoustic streaming induced by traveling surface acoustic waves. (c) Experimental results showing fluorescein isothiocyanate (FITC, green) dextran can be delivered to HeLa cells. The 4,6-diamidino-2-phenylindole (DAPI, blue) stain is used for the cell nucleus. The Alexa 594 red stain is used for indicating dead cells. (a-c) Reproduced with permission.[180] 2021, Processes.